Petrochemistry of Some Gem-Related Metamorphic Rocks in Sri Lanka

Mr. Nuttee Shitangkool

A Report in Partial Fulfillment of the Requirements for the Degree of the Bachelor of Science, Department of Geology,

Chulalongkorn University

2009

ศิลาเคมีของแปรที่สัมพันธ์กับอัญมณีบางบริเวณในประเทศศรีลังกา

นาย นัทธี ชิตางกูร

รายงานฉบับนี้เป็นส่วนหนึ่งของการศึกษาตามหลักสูตรปริญญาตรี

สาขาวิชาธรณีวิทยา ภาควิชาธรณีวิทยา คณะวิทยาศาสตร์

จุฬาลงกรณ์มหาวิทยาลัย

ปีการศึกษา 2552

Date of Submit ……./……../…….

Date of Approval ……./……./…….

……

(Assistant Professor Dr. Chakkaphan Sutthirat)

Senior project advisor

Title	Petrochemistry of Some Gem-Related Metamorphic Rocks in Sri Lanka
Researcher	Mr. Nuttee Shitangkool
Advisor	Assistant Professor Chakkaphan Sutthirat, Ph.D.
Department	Geology
Academic Year	2009

Abstract: Sri Lanka has long been known as the major source of gemstones supplying wide variety, high quality and high quantity to the world market. Gem occurrences in the country are generally related to regional metamorphism. Precambrian high-grade metamorphic rocks have been prospected for gem deposits which are common sources of corundum, tourmaline, chrysoberyl, spinel, zircon, garnet etc**.** Characteristics of some gem-related metamorphic rocks collected from this country were investigated under petrographic description, whole-rock geochemical analysis and mineral chemistry. Rock collections were divided, based on their textures and mineral assemblages, into 6 groups including garnet gneiss, graphitic gneiss, hornblende-biotite gneiss, granulite, mafic granulite and felsic granulite. Moreover, some crucial groups were collected from different localities for comparison such as hornblende-biotite gneiss from Bakamuna and Kadugannawa. In general, petrographic description indicates high grade metamorphic textures, particularly mosaic suture and triple junction. Various minerals are present in different rock types; however, common assemblage usually contains plagioclase, alkali feldspar, quartz, garnet, pyroxene, hornblende and biotite with different proportions; moreover, sillimanite, rutile and opaque minerals may be found as accessory in some groups. Whole-rock geochemistry shows that most of all samples are peraluminous composition, except only a sample of mafic granulite from Bakamuna is metaluminous. Mineral chemistry of some crucial minerals was analyzed for comparison and reconstruction of P-T history of these rocks. As a result, garnet composition is mostly almandine garnet. Pyroxene can be divided to orthopyroxene with significant ferosilite composition and clinopyroxene with composition varying from diopside to hedenbergite. For feldspar, estimated temperature of crystallization appears to be an above 445-550 °C based on compositions of two feldspar presented within the same sample.

หัวเรื่อง	ศิลาเคมีของหินแปรที่สัมพันธ์กับอัญมณีบางบริเวณในประเทศศรีลังกา
ผู้วิจัย	นาย นัทธี ชิตางกูร
อาจารย์ที่ปรึกษา	ผู้ช่วยศาสตราจารย์ ดร. จักรพันธ์ สุทธิรัตน์
ภาควิชา	ธรณีวิทยา
ปีการศึกษา	2552

บทคัดย่อ: ประเทศศรีลังกาเป็นประเทศที่มีชื่อเสียงด้านแหล่งอัญมณีที่สำคัญแห่งหนึ่งของโลก การกำเนิดของอัญมณีในพื้นที่พบว่ามีความสัมพันธ์กับการแปรสภาพของหินแปรในยุคพรีแคมเบรียน ซึ่งอัญมณีที่พบในบริเวณนี้ได้แก่ คอรันดัม คริสโซเบริล การ์เนต สปิเนล ทัวร์มาลีน เซอร์คอนและอื่นๆ โดยหินแปรที่สัมพันธ์กับอัญมณีเหล่านี้ได้ถูกนำมาศึกษาลักษณะต่างๆภายใต้กล้องจุลทรรศน์แสงโพลาไรซ์ วิเคราะห์องค์ประกอบทางเคมีของหินทั้งก้อน และการศึกษาเคมีแร่ ตัวอย่างหินทั้งหมดสามารถแบ่งออกเป็น 6 กลุ่ม ได้แก่ การ์เนตไนส์ แกรฟิติกไนส์ ฮอร์นเบลนด์ไบโอไทต์ไนส์ แกรนูไลต์ เมฟิกแกรนูไลต์และเฟลสิกแกรนูไลต์ นอกจากนี้ หินบางกลุ่มได้ทำการเก็บมาจากต่างพื้นที่เพื่อที่จะนำมาเปรียบเทียบความแตกต่าง เช่น แกรฟิติกไนส์จากบากามุนาและรัตนปุระ

จากการศึกษาศิลาวรรณนาพบว่าลักษณะต่างๆโดยทั่วไปบ่งชี้ถึงการแปรสภาพของหินแปรขั้นสูง โดยเฉพาะอย่างยิ่ง ลักษะขอบผลึกที่เป็นโมเสกและรอยประกบสามเหลี่ยม และแร่องค์ประกอบที่พบในแต่ละตัวอย่างนั้นมีความคล้ายคลึงกัน แต่อาจจะแตกต่างในเรื่องของสัดส่วนและลักษณะบางอย่าง โดยแร่ที่พบทั่วไปได้แก่ แพลจิโอเคลส อัลคาไลเฟลด์สปาร์ ควอรตซ์ การ์เนต ไพรอกซีน ฮอร์นเบลนด์ และไบโอไทต์ นอกจากนี้ยังมีแร่รองต่างๆที่พบได้แก่ ซิลลิเมไนต์ รูไทล์และแร่ทึบแสงเป็นต้น จากการศึกษาธรณีเคมีของหินทั้งก้อนพบว่า ตัวอย่างหินเกือบทั้งหมดมีปริมาณอะลูมิเนียมสูงมาก ยกเว้นเมฟิกแกรนูไลต์เพียงตัวอย่างเดียวจากบากามุนาที่มีปริมาณปานกลาง

จากการศึกษาเคมีแร่ ในกลุ่มแร่การ์เนตพบว่าส่วนใหญ่มีองค์ประกอบหลักเป็นแอลมันดีนการ์เนต ในกลุ่มไพรอกซีนพบว่า มีทั้งที่เป็นไคลโนไพรอกซีนและออร์โธไพรอกซีน โดยในไคลโนไพรอกซีนมีองค์ประกอบทั้งที่เป็นไดออปไซด์และฮิเดนเบอร์ไกต์ ส่วนในออร์โธไพรอกซีนมีองค์ประกอบเป็น ฟอร์โรซิไลต์เท่านั้น สำหรับกลุ่มแร่เฟลด์สปาร์ โดยใช้เฟสไดอะแกรมในการประมาณอุณหภูมิในการสร้างผลึกของแร่นี้ควรสูงกว่า 445-500 องศาเซลเซียส ตามองค์ประกอบของคู่แร่เฟลด์สปาร์ที่พบในหินก้อนเดียวกัน

Acknowledgements

I would like to deeply thank Assist. Prof. Dr. Chakkaphan Sutthirat, my advisor who has supervised throughout this study. Mrs. Malatee Taiyaqupt, Mr. Prachin Thongprachoom and Miss Sopit Poompoung for their generous supported in laboratories. Geologist and gemologist team of the Gem and Jewelry Institute of Thailand (Public Organization) for my study rock samples. I also extend my thanks to department of geology's staffs, my senior, friends and juniors to their suggestion and assistances.

Finally, this paper could not be accomplished without all lecturers of Department of Geology, Faculty of Science, Chulalongkorn University who have been giving me knowledge, experience, suggestion and support.

Contents

List of Figures

List of Tables

CHAPTER I

INTRODUCTION

CHAPTER I

INTRODUCTION

1.1 General Statement

Sri Lanka Island has long been known as the world crucial source of gemstones with good quality, wide variety and high abundance. The island is located in the south of India in which Palk Strait situates between both countries. Sri Lanka and India were parts of the Gondwana Supercontinent in Precambrian before they had early rifted apart since Jurassic. Subsequently, that tectonic event caused complete separation between Sri Lanka and India continent in early Cretaceous (Katz, 1987 cited in Katz et al., 2000). Consequently, most areas in Sri Lanka have metamorphic belts comparable to those expose in East Africa, Madagascar, India and East Antarctica that have been known as Mozambique metamorphic belt

More than 90% of Sri Lanka Island is occupied by Precambrian metamorphic rocks; only the north and north-western parts are covered by Jurassic and Miocene to Quaternary sedimentary rocks. The metamorphic rocks have been subdivided into 3 major units including Wanni Complex (WC), Highland Complex (HC) and Vijayan Complex (VC) (Kroner et al., 1991 cited in Tennakoon et al., 2005). The contact zones between Vijayan Complex and Highland Complex are significantly recognized as flat-lying thrust zones in which are often related to gem deposits, particularly corundum, chrysoberyl, garnet, spinel, tourmaline, zircon etc. (Tennakoon et al., 2005).

However, localities of gem deposits usually situated in the secondary deposits related to primary deposits of the rock occurrences. Research on gems-related metamorphic rocks in these areas would be very useful for further exploration of gem deposits in this country and other countries in which Mozambique belt occurs such as East African countries and Madagascar. Besides, understanding rock compositions and their metamorphism would be crucial information to indicate occurrences of gem variety of Sri Lanka.

1.2 Hypothesis

The gem-related rocks in Sri Lanka have some specific characteristics that can generate gem varieties.

1.3 Problem Defined

Many rock types occurred in Sri Lanka have a close relation to the origin of gem varieties. This research project is therefore designed to investigate petrochemical characteristics of rock samples prior to reconstructing the compositions of protolith. In addition, metamorphism, significant process to produce gem deposits, should also be interpreted to understand the origin of some gem variety in Sri Lanka.

1.4 Objectives

The main objective of this research project is to investigate petrochemistry of some gem-related rocks in Sri Lanka.

1.5 Theoretical Backgrounds and Relevant Researches

Sri Lanka is an important gem deposit of the world. It contains a wide variety of gem with high quality and quantity. Katz (1972, cited in Katz et al., 2000) reported that the metamorphic belt appears to have been caused by tectonic processes, particularly subduction, of the regional terranes. During Precambrian period, many tectonic plates and microplates (e.g., India, Sri Lanka, East Africa, Madagascar, Australia and Antarctica) were merged together in the eastern part of Gondwana (Kart, 1996 cited in Katz et al., 2000) when they had been undertaken metamorphism leading to a high-grade metamorphic belt of amphibolite-granulite facies which are known as Mozambique belt. Subsequently, these plates were moved apart to their recent positions; however, remnants of the Mozambique belt still expose in some parts of these plates.

General geology of Sri Lanka can be subdivided into two periods. Jurassic and Miocene to Quaternary sedimentary rocks with majority of limestone expose restrictively in the northern and northwestern parts of the Island. On the other hand, Precambrian metamorphic rocks of amphibolite to granulite facies occupy widely throughout the country. These metamorphic rocks can be subdivided, based on lithology and tectonic, into three units such as Wanni Complex (WC) mainly in the western and northwestern part, Highland Complex (HC) in the central belt and Vijayan Complex (VC) in the eastern island. In addition a contact belt between Wanni Complex and Highland Complex has been suggested to be a new unit called Kadugannawa Complex (KC) (Kroner et al., 1991 cited in Tennakoon et al., 2005).

Highland Complex, occupying the widest area, consists of about 50% metasediments and 50% metaigneous gneisses (Kroner et al., 1991 cited in Tennakoon et al., 2005). These

rocks are metaquartzites, forsterite marbles, scapolite-wollastonite granulites, garnet-sillimanite-graphite gneisses, garnet-quartz-feldspar granulites which belong to upper amphibolite to granulite facies.

Vijayan Complex is located in the east of HC. Its metamorphic grade is mainly characterized by amphibolite facies. Rocks consist mainly of hornblende-biotite orthogneisses and granitic-granodioritic. These rocks do not seem to have shared the granulite facies condition of the adjacent HC. The contact between HC and VC is interpreted as being a flat-lying thrust zone, along which HC has been thrust southeastwards over the VC (Cooray, 2000 cited in Tennakoon et al., 2005).

Sri Lanka gem occurrences have specific process distinguishable from the other places in the world. For example, corundum deposits locally in marbles are known in many countries including Vietnam, Burma, Kashmir, Afghanistan and Tanzania. The formation of these deposits can be explained by 3 processes below (reviewed by Fernando et al., 2005).

1. Metamorphism of the limestone primarily contaminated by aluminous products of weathering (Okrusch et al., 1976; Rossovskiy et al., 1982).
2. Metasomatic transformations of terregenous layers in marbles by metamorphic solution (Dmitriev, 1982; Kisin, 1991).
3. An influx of Al into marbles by endogenic solutions relates to the alkali magmatism (Terekhov et al., 1999).

However, Fernado et al. (2005) reported that marble-hosted corundum deposits in Sri Lanka have somehow different process as mentioned above. These corundums are found in lenticular layer between marble and pelitic gneisses. Mineral reaction zones, therefore, appear to have occurred along the contact of marble and pelitic gneisses which show various textures ranging from fine-grained, equigranular to coarse-grained rocks. Three distinctive mineralogical zones are recognized as present below.

Marble	*Spl + Phl* *(Zone 1)*	*Crn + Phl* *(Zone 2)*	*Crn + An* *(Zone 3)*	High Grade Pelitic Gneiss

Alteration features resulted from heat sources have been reported in each zone. The succession of alteration zones, under thin-section study, is present below.

	Country Rock	Reaction Bands			Country Rock
Stage 1	Marble	*Spl + Phl*	*Crn + Phl*	*Crn + An*	Pelitic Gneisses
Stage 2		*Taaf*	*Neph + Alb*	*Scap*	
Stage 3		*Scheelite*			
Stage 4		*Chl + Mus + Cal*			

Mineral abbreviations: Phl-phlogipite, Crn-corundum; Spl-Spinel; Scap-scapolite; Neph-nepheline; Taff-Taaftaaffeite; Alb-Albite, Mus-muscovite, Chl-chlorite, Cal-Calcite, An-Anorthite

Therefore, the other types of gem deposits in Sri Lanka may also have specific characteristics that can in turn be important data obtained from this research.

1.6 Scope of Work

In this study, polished-thin sections were prepared for petrographic description, particularly for metamorphic textures and mineral compositions, which were initially carried out using polarizing microscope. Electron Probe Micro-Analyzer (EPMA) was subsequently engaged to analyze mineral chemistry of significant assemblages of selective rock samples. Whole-rock geochemical analysis was carried out using X–Ray Fluorescence (XRF) Spectrometer for major and minor elements.

1.7 Methodology

Methods of this study are summarized as a schematic flowchart in Figure 1.1 and their details are reported below.

Literature Reviews: previous works and relevant researches were firstly reviewed to know geologic setting and nature of gem deposits of the study area; besides, they were extracted for some theoretical background and analytical framework to support this study.

Sample Collection and Classification: rock samples under this study were provided by the Gem and Jewelry Institute of Thailand (Public Organization) (GIT). These samples were roughly identified and grouped into 6 groups based on features and their textures.

Sample Preparation: was divided into 2 procedures. Thin and polished-thin sectioning was done for microscopic investigation and EPMA analysis. The second procedure was rock powdering for whole-rock geochemical analysis.

Petrographic Description: mineral assemblage and metamorphic texture in each rock group were described under a polarizing microscope (Figure 1.2); subsequently, particular samples were selected for EPMA and whole-rock geochemical analyses.

EPMA Analysis: was planned to analyze the selective polished-thin sections of particular rock samples for mineral chemistry using an Electron Probe Micro-Analyzer (EPMA) model JXA-8100 (Figure 1.3). Total 10 samples including 8 polish-thin sections and 2 polished sections were analyzed, consequently. The EPMA used under this study is based at the Geology Department, Faculty of Science, Chulalongkorn University. Mineral and pure oxide standards were used for calibration of quantitative analysis and operating conditions were set at 15 kV and about 2 μA with focused beam smaller than 1 μm in diameter.

Whole-Rock Geochemical Analysis: was planned for major and minor element compositions of rock samples using X-ray Fluorescence Spectrometer (XRF) model S-4 Pioneer (Figure 1.4) based at Faculty of Science, Chulalongkorn University. Press powder method was applied with analytical condition of maximum rating ≤ 4 kV, 50 Hz and 8 kvA. Internal standards were applied for calibration the analytical results. In addition, loss on ignition (LOI) was separately analyzed to analyze the valentine content and to check quality of the XRF analyses.

Data Verification: all EPMA and XRF results were verified during the study leading to repletion of analysis as appropriate for some samples. Qualified data were then selected for interpretation and further discussion.

Interpretation, Discussion and Conclusion: all results were finally used for interpretation and discussion particularly on petrogenesis as well as protolith and metamorphism. Conclusions were subsequently made in particular aspects including recommendations.

Report Writing and Presentation: full research report was written up and submitted to the Geology Department to fulfill the requirement of BSc (Geology) program whereas presentation was also done in the department seminar. Moreover, short technical paper may be drafted for further publication.

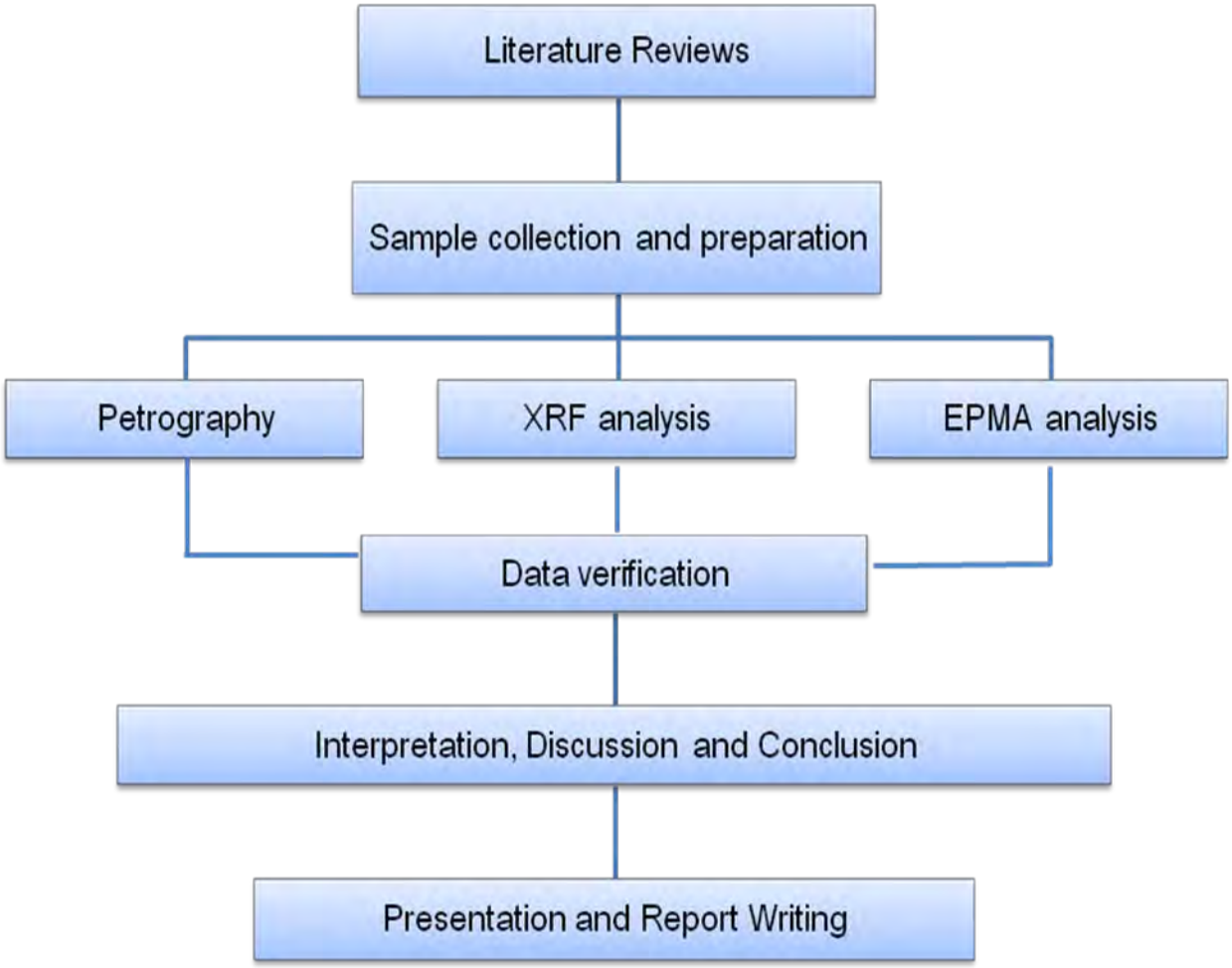

Figure 1.1 Schematic diagram showing methods of this study.

Figure 1.2 Polarizing Microscope based at the Geology Department, Chulalongkorn University used for petrographic works.

Figure 1.3 Electron Probe Micro-Analyzer (EPMA) (JEOL model JXA-8100) based at Department of Geology, Faculty of Science, Chulalongkorn University applied for analysis of mineral chemistry.

Figure 1.4 X-Ray Fluorescence Spectrometry (Model Bruker axs S-4 Pioneer) based at Faculty of Science, Chulalongkorn University applied for whole-rock analysis.

CHAPTER II

GEOLOGIC SETTING AND GEM DEPOSITS IN SRI LANKA

CHAPTER II

GEOLOGIC SETTING AND GEM DEPOSITS IN SRI LANKA

2.1 Geological Setting

Sri Lanka forms a small but very important jigsaw piece of the Gondwana supercontinent. The Gondwana (Figures 2.1 and 2.2) had been marked by collision event between the component cratons of West Gondwana (e.g., Africa and South America) and East Gondwana (e.g. Australia, Antarctica, India, Sri Lanka and Madagascar) when they had been undertaken metamorphism leading to a high-grade metamorphic belt of amphibolite-granulite facies which are known as Mozambique belt. Subsequently, these plates were moved apart to their recent positions; however, remnants of the Mozambique belt still expose in some parts of these plates (Wilson et al., 1997).

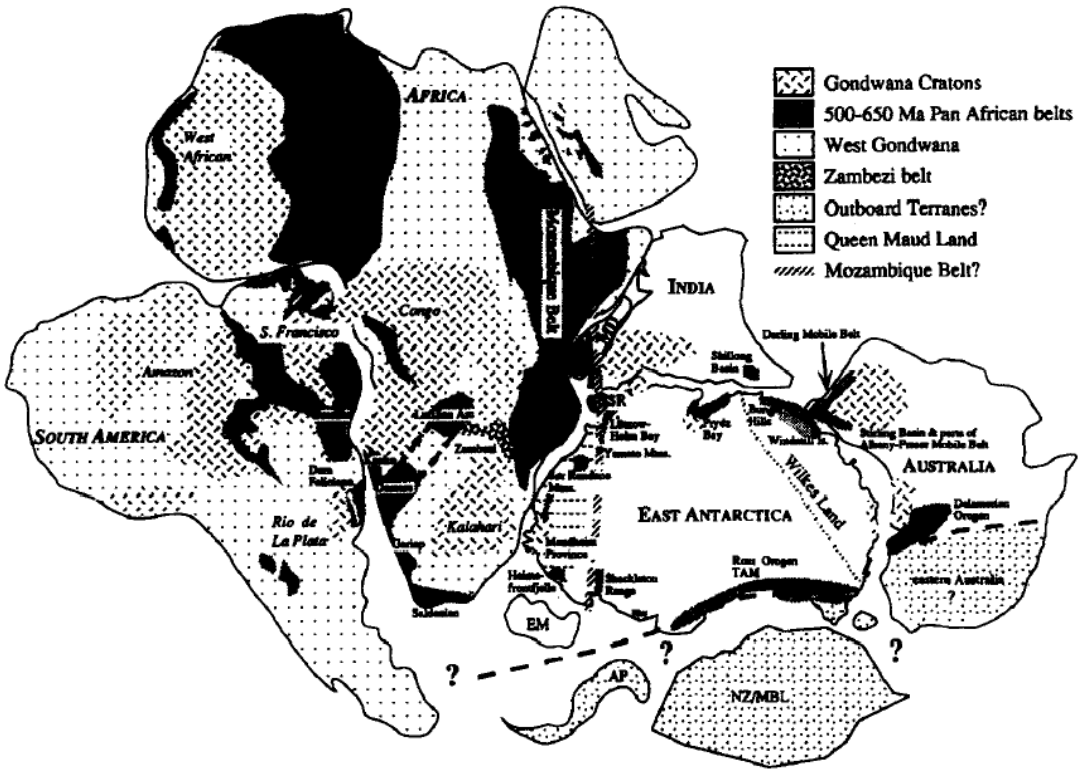

Figure 2.1 Reconstruction of Gondwana after Lawver and Scotese (1987) and Grunow (1995). AP, Antarctic Peninsula; EM, Ellsworth Mountains; MD, Madagascar; NZ&IBL, New Zealand/Marie Byrd Land; QML, Queen Maud Land; SR, Sri Lanka; TAM, Transantarctic Mountains (cited in Wilson et al., 1997).

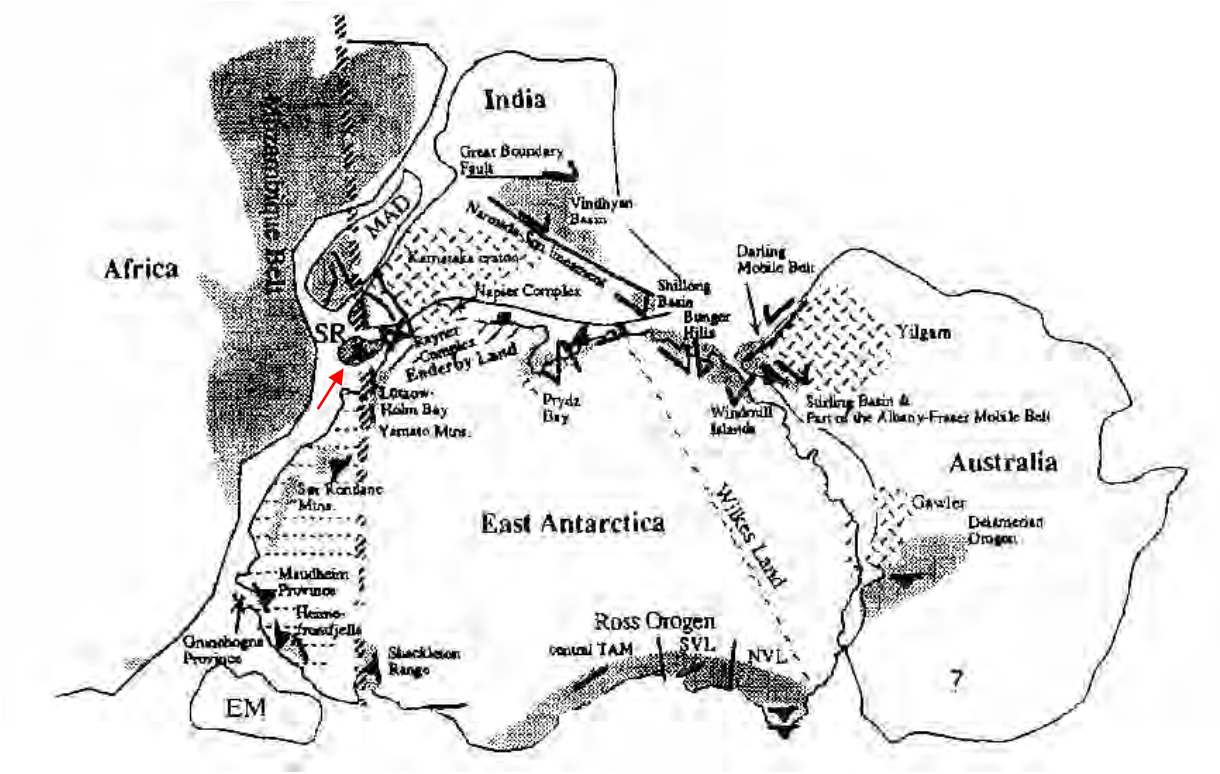

Figure 2.2 Location and structural kinematics of 650-500 Ma tectonism in East Gondwana. Inferred continuation of the Mozambique belt shown crossing East Antarctica. Abbreviations are the same as in Figure 2.1 except for NVL, northern Victoria Land; SVL, southern Victoria Land (Wilson et al., 1997). The red arrow indicates location of Sri Lanka.

More than 90% of the Sri Lanka Island is underlain by Proterozoic high grade metamorphic rocks of amphibolite to granulite facies occupying widely throughout the country (Figure 2.3). On the other hand, Jurassic and Miocene to Quaternary sedimentary rocks with majority of limestone expose restrictively in the northern and northwestern parts of the Island. These metamorphic rocks of Sri Lanka can be subdivided into three units, based on lithology and tectonic (see Table 2.1), such as Wanni Complex (WC) mainly in the western and north-western part, Highland Complex (HC) in the central belt and Vijayan Complex (VC) in the eastern island. In addition, a contact belt between Wanni Complex and Highland Complex has been suggested to be a new unit called Kadugannawa Complex (KC) (Kroner et al., 1991 cited in Tennakoon et al., 2005).

Figure 2.3 Geological map of Sri Lanka. Geographical coordinate are Latitude N9°50 - N5°50, Longitude E79°30 - E82°00, Scale 1: 500,000 (Cooray, 1982). Available at library.wur.nl/WebQuery/isric/20944. King Abdul Aziz University, Jiddah, Kingdom of Saudi Arabia.

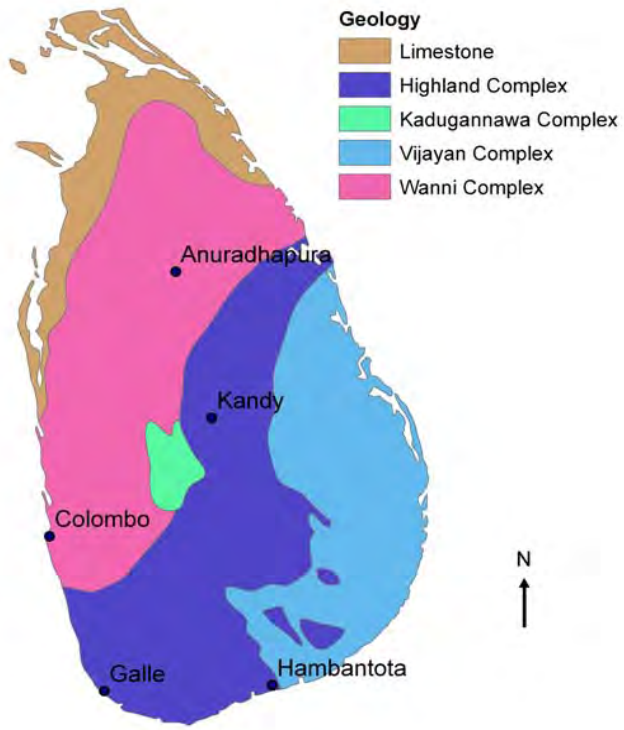

Figure 2.4 Simplified geological map of Sri Lanka showing the major geological units and locations of some crucial cities (after Sansfica, 2008).

Highland Complex (HC): is centrally located with NE-SW trending belt (Figure 2.4) which comprises mainly charnockitic gneisses and granulites, metasediments, basic granulites, gneisses and migmatites. In addition, metasediments including quartzites, marbles, pelitic gneisses and garnet-sillimanite schist (also known as Khondalites) are also recognized in this complex. The crucial prograde, *in-situ* charnockitisation, phenomenon firstly discovered in the Kurunegale area (now included within the Wanni Complex) is also seen in a number of localities in the HC terrane (e.g., Digana and Habarana) (Cooray, 2000 cited in Tennakoon et al., 2005).

In the southwestern parts of the HC, thick bands of marble and quartzite are rare but there are many bands of wollastonite-scapolite, diopside-scapolite rocks and cordierite-bearing gneisses, instead. This lithological difference used to be a criterion for subdivision of the central belt into two units, Highland Group and Southwestern Group (Cooray, 1962, 1984; Katz, 1972b cited in Mathavan et al., 1998). However, this lithological difference is now attributed to a change in the sedimentary facies; consequently, the whole belt is now considered as a single unit that underwent similar geological history.

Vijayan Complex (VC): As compared to the HC, detailed information, particularly on geological structure, geochronology and field relations are lacking on the Vijayan rocks. This unit consists mainly of microcline-bearing granitic gneiss, hornblende-biotite gneiss and migmatite and minor quartzite and calc-silicate rocks. In addition, a few inliers, consisting of typical HC rocks, occur within the VC. Absence of muscovite, almandine garnet and aluminosilicates is notable. These rocks do not seem to have shared the granulite facies condition of the adjacent HC. The contact between HC and VC is interpreted as being a flat-lying thrust zone, along which HC has been thrust southeastwards over the VC (Cooray, 2000 cited in Tennakoon et al., 2005).

Wanni Complex (WC): consists mainly of leucocratic gneisses and migmatites, which range in composition from granitic to tonolitic and charnockitic gneisses. Metasediments are relatively less abundant but cordierite bearing gneisses and migmatites are ubiquitous in the Colombo and Gampha areas. Late microcline-bearing alkaline rocks are relatively more common than in the other two units. Some workers have subdivided the WC into two sub-units, i.e., the Eastern Highland Complex (areas lying within former Highland Group) and the Western Granite Gneiss (areas representing former Western Vijayan Series).

Grade of metamorphism of the Wanni Complex rocks ranges from upper amphibolite to granulite facies, but a regional prograde relation is not recognized. These rocks show widespread retrogression in areas that have undergone granulite facies metamorphism clearly seen in several quarries from Kurunegale to Puttalam.

Table 2.1 Geochronological framework for the high-grade rocks of Sri Lanka (after Kroner and Williams, 1993, cited in Mathavan et al., 1998)

	WC (Ma)	HC (Ma)	VC (Ma)
Depositional age of supracrustal rocks	-2000	-1100	-1100
Granitoid intrusives	0665-1942	-770-1100	-1000-1100
Regional granulite- grade metamorphism	<665>540	<665>540	
Regional amphibolite - grade metamorphism			-465-558
In-situ charnokitization	-550	535-550	
Post-tectonic granites	-550-580	-550	
Cooling	463-611	420-524	

2.2 Gem Deposits

Most of Sri Lankan gem deposits located on a high pressure zone in the southeastern and northern parts of the island, particularly along the Highland Complex. The metamorphism temperature of the Highland Complex was appears to rise up to about 700 to 900 °C (Prame, 1991 cited in Dissanayake et al., 2000). In addition, low pressure gem deposits are rarely or not composed of pyroxene±garnet bearing rocks.

As mentioned above, gem deposits of Sir Lanka mainly locate on the Highland Complex that had been metamorphosed to granulite facies. On the other hand, gem deposits found in Vijayan Complex seem to have been transported via the rivers running from Highland complex.

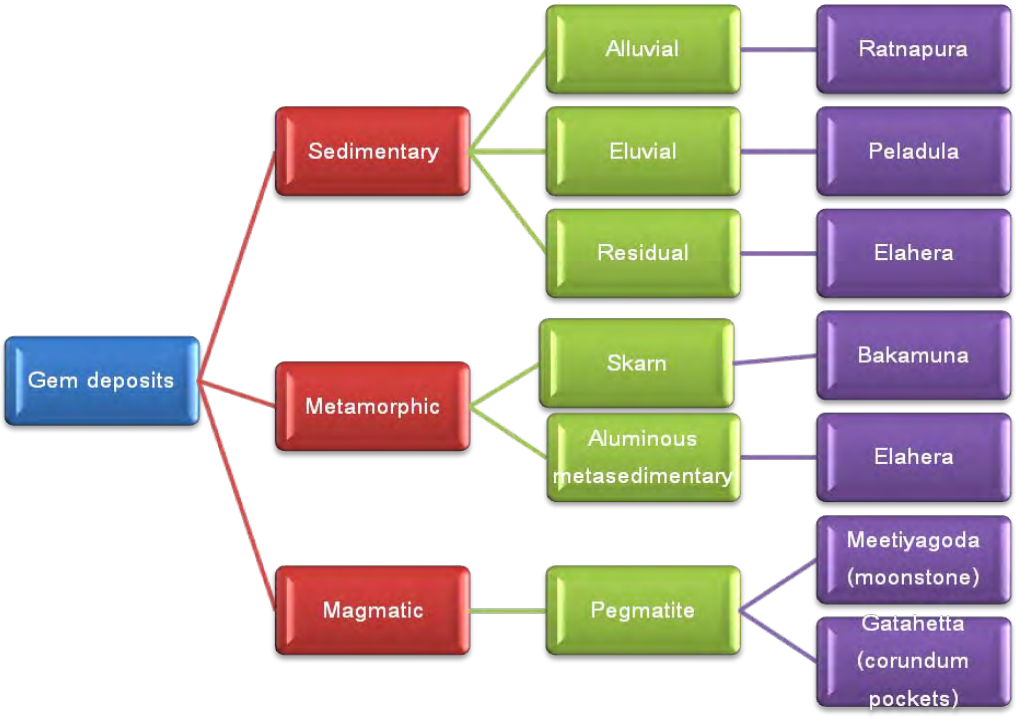

Figure 2.5 Classification of gem deposit in Sri Lanka and their examples of location (Dissanayake and Rupasinghe 1995, cited in Dissanayake et al., 2000)

Classification of gem deposits in Sri Lanka was suggested by Dissanayake and Rupasinghe (1995, cited in Dissanayake et al., 2000) based on lithology of the gem-bearing rocks. These help to predict economic value of potential areas. Specific deposit types and examples are summarized in Figure 2.5.

Sedimentary gem deposits: are the most important locations and have high economic value in Sri Lanka. They can be divided into three types of deposits (Dissanayake et al., 1980, cited in Dissanayake et al. 2000) such as residual, elluvial and alluvial deposits. The characteristics of these gem deposits are thin layers or lense that consist of rock fragment or sand, known as *"Illam"*, deposit along rivers, alluvial plains, hillslopes and hillsides.

Residual gem deposits occur from *in-situ* weathering and found at depth ranging from few centimeters to about 10 meters. They may form in old flood plain of the stream assumable to nearly source rocks. The indicator might be the layer of alternating sand clay or laterite that consists of angular fragment. The good example of these gem deposits is Elahera.

Elluvial gem deposits are usually found along hillslope and flat areas between the valleys. They have been graded to the alluvial deposits where clear identification is difficult. The characteristic features of the elluvial gem deposits are angular to sub rounded sediments.

Alluvial gem deposits contain the widest varieties of gem minerals in Sri Lanka. The best example is located in Ratnapura. The gem-bearing layers were found at depth about 20 meters and possibly composed of two or three layers. The characteristic features of gems and rock fragment were more rounded than those of the elluvial deposits. This deposit type occurred in old flood plain or stream.

Metamorphic gem deposits: is the most crucial gem deposit in Sri Lanka that is agreeable to the fact that Sri Lanka has high grade metamorphic rocks covering about 90% of the whole area. The metamorphic gem deposits can be subdivided in to two rock types: 1) skarn and calcium-rich rocks; 2) alluminous metasedimentary rocks.

Maesschalck and Oen (1989, cited in Dissanayake et al., 2000) studied the fluid inclusions in corundum from skarn and calcium-rich rocks in Sri Lanka and reported CO_2 inclusion. CO_2 is an important indicator for gem occurrences. These primary fluids suggest the temperature of corundum forming under condition of granulite facies (> 630 ºC, 5.5 kbar) whereas the secondary fluid inclusions indicate retrograde post-metamorphic cooling and uplift of these areas. In addition, density of the fluid inclusions (average density, d = 1.05 g/cm^3) also suggest that the formation of corundum are under granulite facies. Silva and Siriwardena (1988 cited in Dissanayake et al., 2000) described an example of a corundum-bearing skarn deposit, located at Bakamuna near the main Elahera gem field. Cooray (1984) and Wadia and Fernando

(1945) (cited in Dissanayake et al., 2000) described some more examples of this type at Elahera and at Ohiya, respectively.

Alluminous metasedimentary rocks found are part of abundant metasedimentary rocks found in HC. Characteristic and chemical compositions suggest the suitable condition to the origin of gem, particularly the aluminous gem mineral. Katz (1986, cited in Dissanayake et al., 2000) suggested that these gemstones have an origin related to granulite facie involving CO_2 flooding, purging of H_2O-rich fluid and partial melting. Cooray and Kumarapeli (1960, cited in Dissanayake et al., 2000) studied the occurrence of corundum in biotite-sillimanite gneiss and described its recrystallization belongs to the formation of aluminium-rich, silica-poor bands in a semipelitic gneiss.

Magmatic gem deposits: Pegmatites are generally found in the Highland Complex and they are also considered as an important source of gem minerals. The best known pegmatitic gem deposit is moonstone deposit at Meetiyagoda, southern of Sri Lanka (Spencer 1930 and Malley 1989, cited in Dissanayake et al. 2000). The moonstones have been located in the regions around Balangoda and Kundasale near Kandy. Pegmatites in Sri Lanka also contain other gem minerals such as beryl, chrysoberyl, zircon and corundum (Rupasinghe et al., 1994, cited in Dissanayake et al., 2000).

CHAPTER III

RESULTS

CHAPTER III

RESULTS

3.1 Sample Collection

All the samples collected for this study were provided by the geologist and gemologist team of the Gem and Jewelry Institute of Thailand (Public Organization). They had collected these rock samples during the fieldtrips in Sri Lanka in 2004 and 2005. Various types of gem occurrence were visited during the trips. Therefore, the rock collection was initially grouped, into 3 areas including Bakamuna (in Highland Complex, HC), Kadugannawa (in Kadugannawa Complex, special formation between Wanni Complex, WC, and HC) and Ratnapura (in HC). Figure 3.1 shows locations of the rock collection and geologic setting.

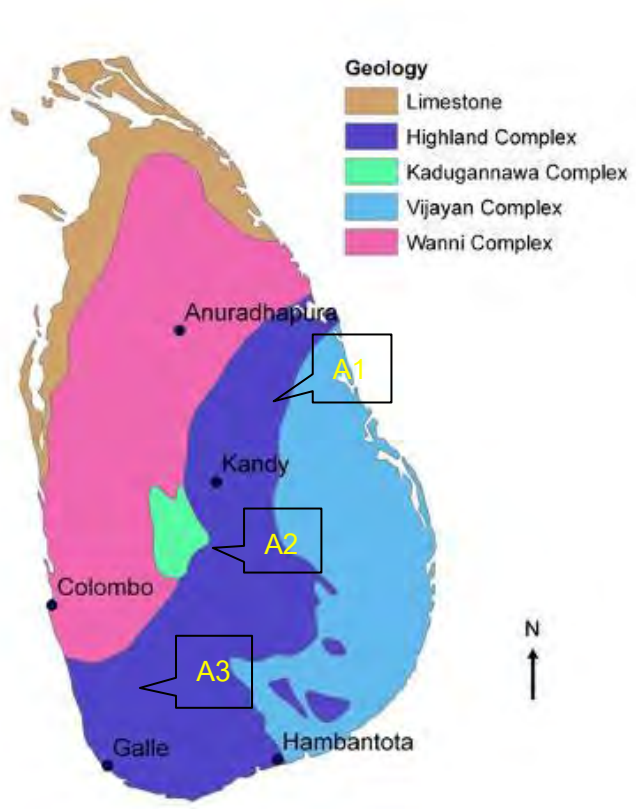

Figure 3.1 Simplified geologic maps (after Sansfica, 2008) showing locations of rock sample collection within 3 areas including:

A1 Bakamuna for sample nos. SL1, SL4, SL5, SL6, SL10 and SL11;

A2 Kadugannawa for sample no SL9;

A3 Ratnapura for sample nos. SL13, SL16 and SL17.

3.2 Petrography

All of rock samples are metamorphic rocks with different appearances that may belong to different metamorphic facies. These samples can be classified into 6 types. The first type (i.e., samples SL1 and SL10) is **Garnet Gneiss** containing red granoblastic garnet and presenting slightly foliation. The second type is classified as **Granulite** (i.e., samples SL4 and SL13) that has 2 essential minerals including feldspar and pyroxene. They show foliation between dark- and light-colored bands. The third type is **Mafic Granulite** which foliation is not well recognized; it contains 2 main mineral assemblages, i.e., pyroxene and garnet (sample SL5). The fourth type is **Graphitic Gneiss** that shows clearly foliation and contains garnet porphyroblast and some graphite in some particular layers (samples SL6 and SL16). The fifth type is **Hornblende-Biotite Gneiss** containing dominantly biotite and hornblende with slight foliation (samples SL9 and SL11). The last type is **Felsic Granulite** containing mainly quartz and some pyroxene without foliation (sample SL17).

For petrographic study, all of the selective rock samples have similar mineral assemblages and textures. Essential minerals often found are quartz, amphibole, pyroxene, garnet, mica, plagioclase, K-feldspar and opaque mineral. Representative hand specimens and photomicrographs of all rock types are shown in Figures 3.2-3.7.

Garnet Gneiss: clearly shows granoblastic texture of garnet, quartz and feldspar (Figure 3.2) which their proportion is of about 45% garnet, 20% quartz, 10% alkali feldspar and small amounts of sillimanite, biotite and opaque mineral. Garnet porphyroblasts usually show anhedral crystal with size ranging from 2-4 mm. Alkali feldspar usually shows perthitic texture and tartar twin with size ranging from 0.2-2 mm. Biotite and sillimanite show unclearly preferred orientation and may form glomerocrysts with size ranging from 0.1-2 mm.

Granulite: shows granoblastic texture of quartz, feldspar, pyroxene forming as essential assemblage (Figure 3.3). Garnet, hornblende and opaque mineral are identified as accessory. Their proportions are of about 35% plagioclase, 30% pyroxene, 10% quartz and 25% accessory. Felsic minerals usually form mosaic with well-developed triple junction that indicates high grade metamorphism. They range in size from 0.2 to 2 cm. Alkali feldspar shows perthitic texture and quartz exsolution (mrymekitic texture) which are subsolidus re-equilibration. Pyroxene usually shows anhedral and relic texture with ranging in size from 0.4-1 mm.

Mafic Granulite: contains porphyroblastic garnet and pyroxene surrounded by groundmass of quartz, plagioclase and opaque minerals (Figure 3.4). Their proportions are of about 45% garnet, 35% pyroxene, 10% quartz, 10% plagioclase and the other. Garnet and pyroxene usually show anhedral-subhedral crystals developing triple junction, crack and relic texture. Their textures indicate high grade metamorphism with ranging in size from 1-5 cm. The other minerals usually form also triple junction along with mosaic texture which range in size from 0.2-1 mm.

Graphitic Gneiss: shows granoblastic grains surrounding porphyroblast of garnet in particular (Figure 3.5). Alkali feldspar and other minerals is granoblastic matrix. Their proportions are of about 55% alkali feldspar, 15% quartz, 10% garnet and 20% of accessory which is typically characterized by biotite and opaque mineral. Garnet usually shows anhedral-subhedral with crack and relic texture; their sizes range from 2-5 mm. In addition, alkali feldspar shows development of mosaic suture and triple junction. Perthitic texture was also found in many alkali feldspar grains ranging size from 0.1-4 mm. Biotite and opaque mineral (likely graphite) usually form lepidoblastic grain ranging size from 0.2-0.5 mm long.

Hornblende-Biotite Gneiss: shows granoblastic texture and some lepidoblastic biotite showing orientation (Figure 3.6). Their mineral assemblage proportions are of about of 40% biotite, 35% hornblende, 20% plagioclase and about 5% of quartz and opaque mineral. Biotite usually shows orientation of lepidoblastic with size ranging from 0.5-3 mm. Hornblende usually shows subhedral-euhedral granoblasts which develop triple junction with grain size ranging from 1-4 mm. Plagioclase (av. 0.2-3 mm) usually shows albite and Carlsbad-albite twining. Vermicular quartz was also found along some grains indicating re-equilibrium process at lower temperature subsolidus.

Felsic Granulite: shows typical granoblastic texture of alkali feldspar, pyroxene and quartz which proportions are of about of 45% alkali felspar, 30% pyroxene and about 25% accessory of quartz and opaque mineral, Ilmenite. Alkali feldspar usually forms anhedral-subhedral granoblast ranging size from 0.2-3 mm with triple junction indicating high grade metamorphism. Pyroxene shows slightly cleavages and cracks; some relic textures are recognized in some crystals. Anhedral-subhedral granoblastic pyroxene range in size from 0.2-1 mm.

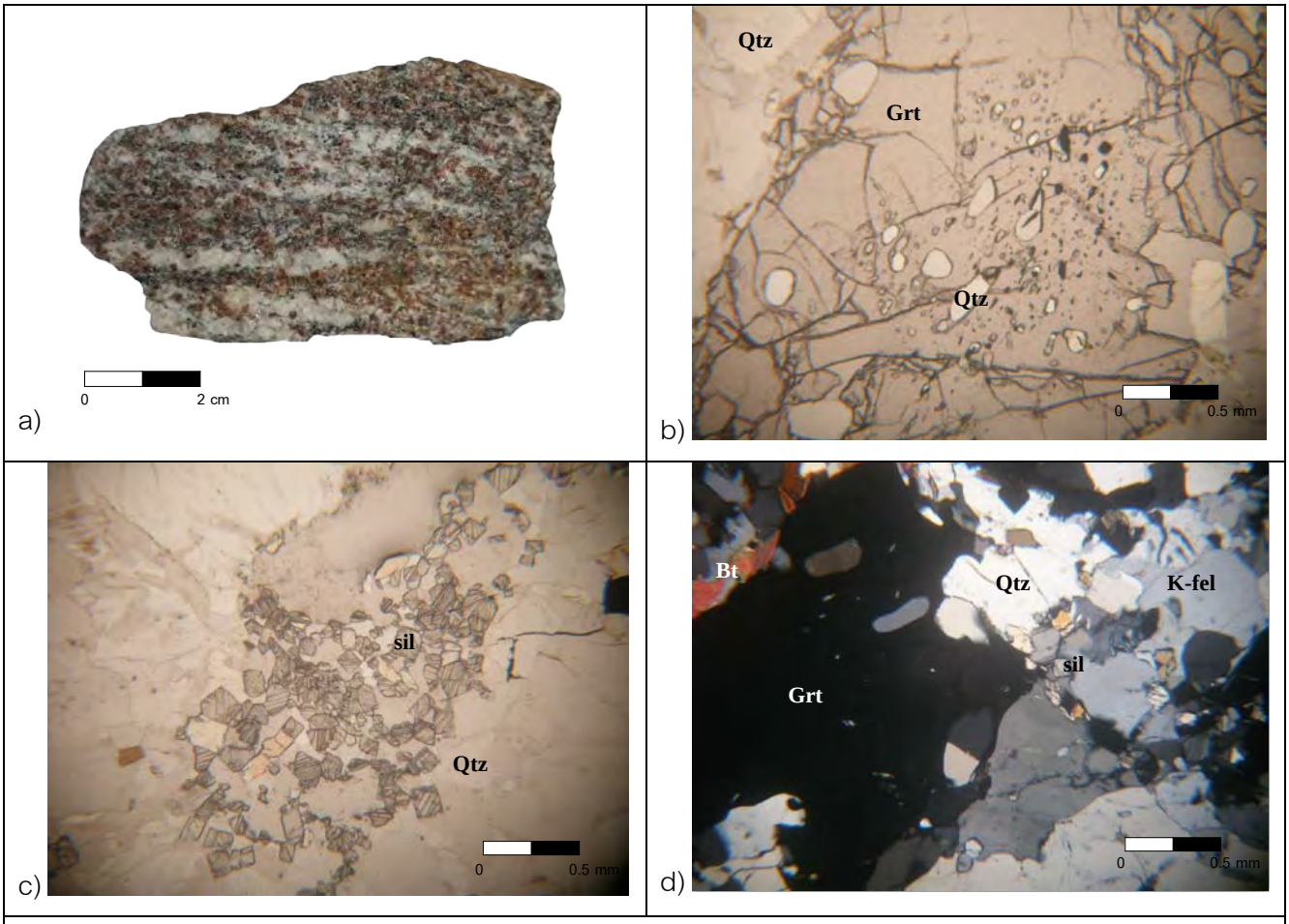

Figure 3.2 Garnet Gneiss (samples SL1 and SL10): a) a slab specimen (SL1) shows foliation and brownish garnet granoblasts; Photomicrographs of b) quartz (Qtz) intergrowth within garnet (Grt) porphyloblastic (SL1, PPL); c) small sillimanite (sil) glomerocrysts (SL1, PPL); d) granoblastic texture of garnet (Grt), quartz (Qtz) and alkali feldspar (K-fel) (SL1, XPL).

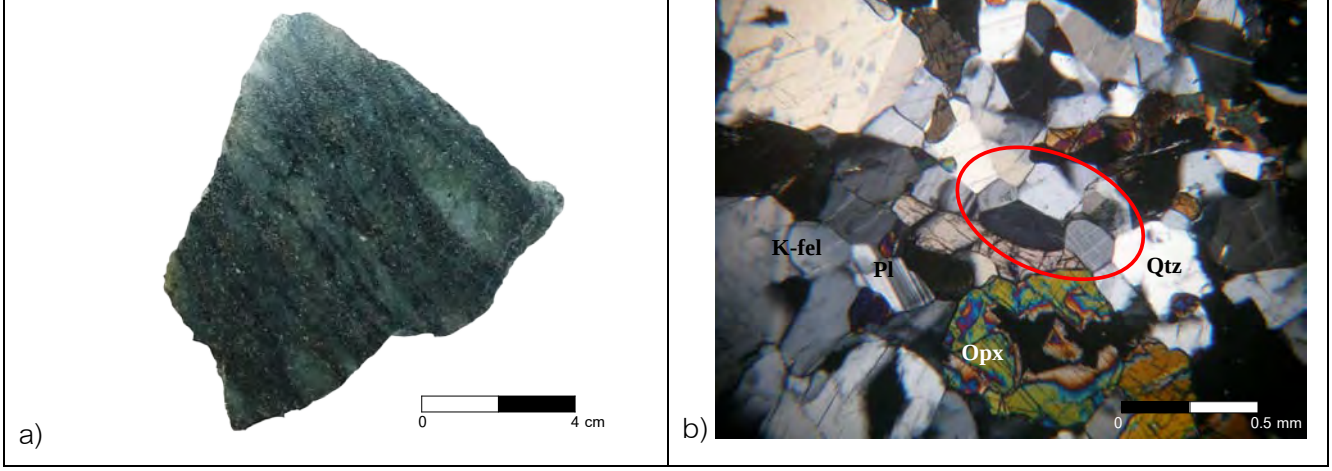

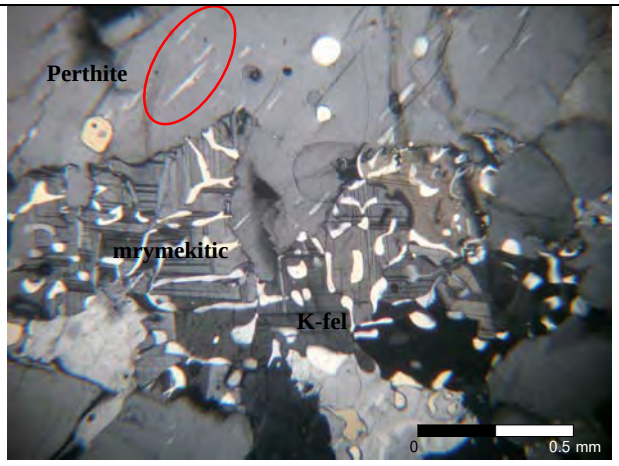

c)

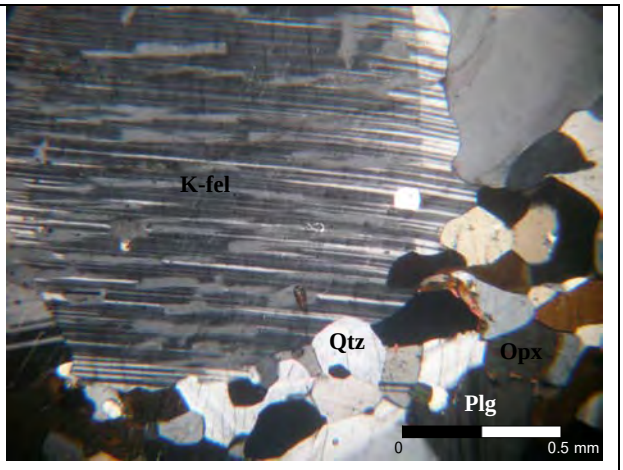

d)

Figure 3.3 Granulite (samples SL4 and SL13): a) slab section showing slightly foliation (SL13); b) recrystalized quartz (Qtz), alkali feldspar (K-fel), plagioclase (Pl) and orthopyroxene (Opx) showing polygon shape with triple junctions (in red circle) (SL4, XPL); c) myrmekitic quartz intergrowth within perthitic (red circle) alkali feldspar (K-fel) (SL13, XPL); d) exsolution of plagioclase (Plg) in alkali feldspar (K-fel) (XPL).

a)

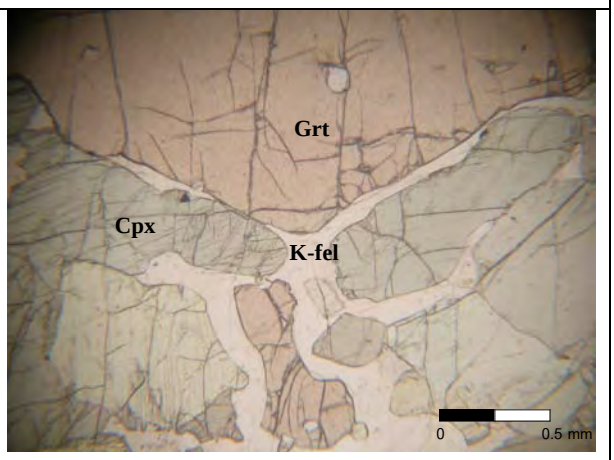

b)

Figure 3.4 Mafic Granulite (sample SL5): a) slab section showing dark mafic minerals without foliation; b) triple junctions between garnet (Grt) and clinopyroxene (Cpx) with replacement of alkali feldspar (K-fel) (PPL).

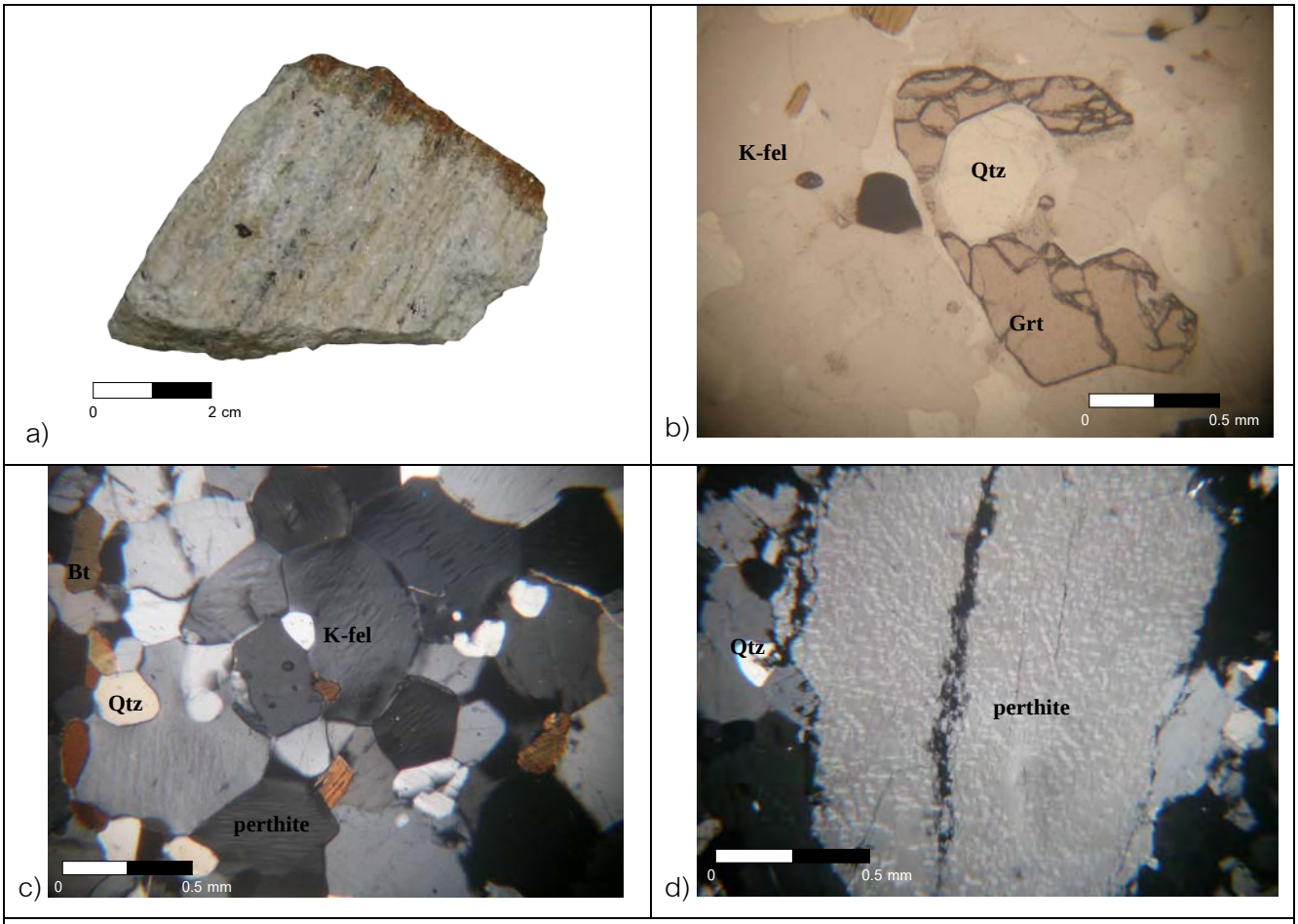

Figure 3.5 Graphitic Gneiss (samples SL6 and SL16): a) specimen showing foliation and garnet porphyloblasts (SL6); b) recrystalized euhedral quartz (Qtz) intergrowth within garnet (Grt) porphyloblasts (SL6, PPL); c) recrystalized quartz (Qtz) and alkali feldspar (K-fel) showing well-developed polygon with triple junction (SL16, XPL); d) Exsolution of albite within a large alkali feldspar grain (perthitic texture) in SL6 (XPL).

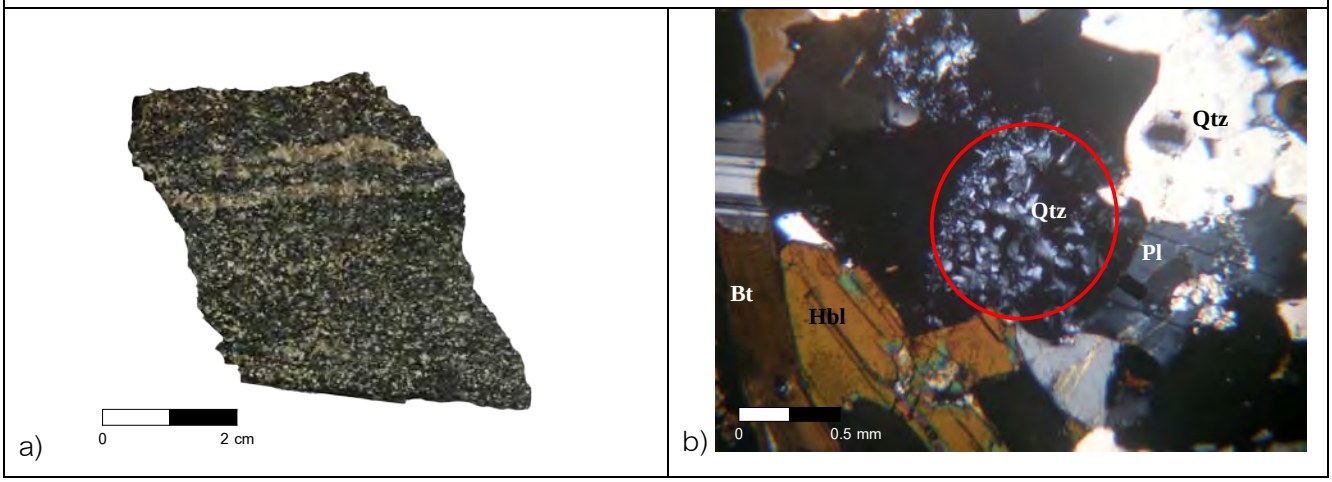

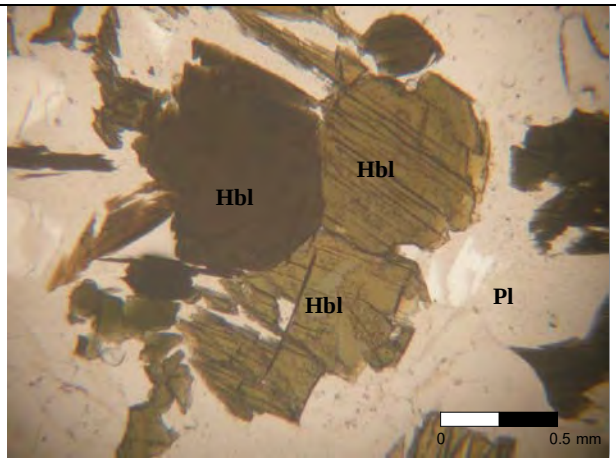

c)

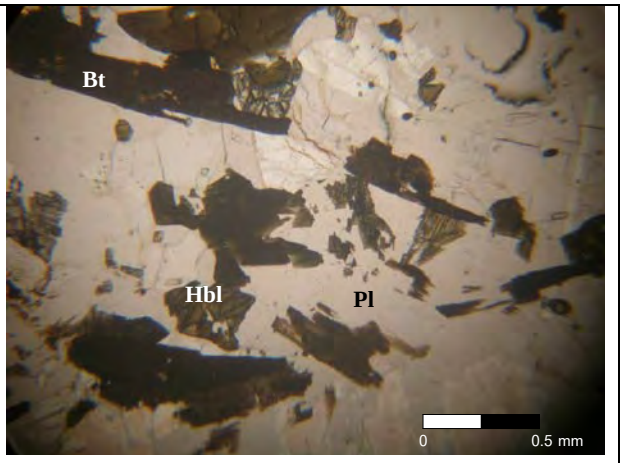

d)

Figure 3.6 Hornblende-Biotite Gneiss (samples SL9 and SL11): a) specimen showing foliation (SL9); b) vermicular texture of quartz (Qtz) indicating disequilibrium process (SL9, XPL); c) triple junction of subhedral hornblende (Hbl) (SL9, PPL); d) orientation of biotite (Bt) and some intergrowth grains with hornblende (Hbl) (SL9,PPL).

a)

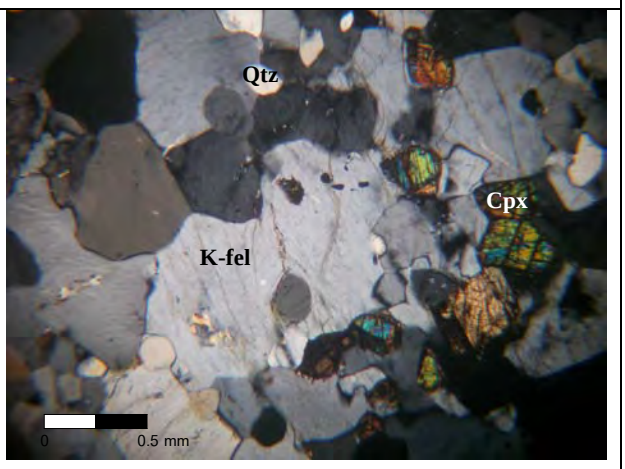

b)

Figure 3.7 Felsic Granulite (sample SL17): a) slab section showing felsic minerals without foliation; b) recrystalized polygonal crystals of quartz (Qtz), alkali feldspar (K-fel) and clinopyroxene (Cpx) with well-developed triple junction, and perthitic texture in K-feldspar (XPL).

3.3 Whole-Rock Geochemistry

Geochemistry was studied to understand the nature of rock that may lead to petrological interpretation. Therefore, geochemical study was carried out in this project. X-ray Fluorescence (XRF) Spectrometer was engaged to analyze major and minor compositions of rock samples. The analyses are reported as major and minor oxides (weight %) including SiO_2, TiO_2, Al_2O_3, Fe_2O_3, MnO, MgO, CaO, Na_2O, K_2O and P_2O_5 in Table 3.3.1. Most of samples are chemically classified as peraluminous rocks except sample SL5 is metaluminous (see Table 3.2).

Table 3.1 Major and minor oxides (weight %) of the selective rock samples analyzed using XRF.

Sample No.	Garnet Gneiss			Graphitic Gneiss			Hornblende-Biotite Gneiss			Granulite			Mafic Granulite	Felsic Granulite
	SL1	SL10	Ave.	SL6	SL16	Ave.	SL9	SL11	Ave.	SL4	SL13	Ave.	SL5	SL17
SiO_2	64.03	68.93	66.48	72.56	71.93	72.25	50.02	49.51	49.77	64.49	65.21	64.85	43.28	70.72
TiO_2	1.00	0.68	0.84	0.41	0.30	0.36	1.79	2.13	1.96	0.56	1.05	0.81	2.49	0.38
Al_2O_3	16.07	16.04	16.06	14.32	14.81	14.57	15.42	15.35	15.39	14.76	13.83	14.30	13.33	13.37
Fe_2O_3	11.05	8.49	9.77	0.50	0.45	0.47	11.66	12.66	12.16	5.72	6.93	6.32	20.57	2.71
MnO	0.26	0.19	0.23	0.00	0.00	0.00	0.21	0.23	0.22	0.09	0.09	0.09	0.31	0.04
MgO	2.48	1.78	2.13	0.00	0.05	0.02	4.82	4.35	4.58	1.50	0.83	1.17	3.89	0.17
CaO	1.02	0.67	0.85	1.59	1.61	1.60	10.08	9.73	9.90	5.08	3.32	4.20	10.45	1.56
Na_2O	1.02	0.64	0.83	3.36	3.48	3.42	3.43	3.58	3.51	3.88	3.12	3.50	2.82	3.07
K_2O	2.57	2.08	2.2	6.64	6.88	6.76	1.73	1.38	1.56	3.26	4.55	3.91	0.94	7.34
P_2O_5	0.08	0.06	0.07	0.17	0.13	0.15	0.64	0.87	0.76	0.08	0.53	0.31	0.39	0.10
LOI	0.33	0.33	0.33	0.32	0.37	0.34	0.69	0.50	0.59	0.27	0.17	0.22	0.07	0.58
Total	99.56	99.56	99.56	99.54	99.64	99.59	99.79	99.79	99.79	99.43	99.47	99.45	98.46	99.46

Table 3.2 Comparison between Na_2O+K_2O and Na_2O+K_2O+CaO to Al_2O_3 for alumina saturation and SiO_2 content for silica saturation

	Sample no.	SiO_2	Na_2O+K_2O	Na_2O+K_2O+CaO	Al_2O_3	Alumina Saturation	Silica Saturation
Garnet gneiss	SL1	64.03	3.59	4.61	**16.07**	Peraluminous	Intermediate
	SL10	68.93	2.72	3.39	**16.04**	Peraluminous	Acidic
Graphitic gneiss	SL6	72.56	9.99	11.58	**14.32**	Peraluminous	Acidic
	SL16	71.93	10.36	11.97	**14.81**	Peraluminous	Acidic
Hornblende-Biotite Gneiss	SL9	50.02	5.16	15.24	**15.42**	Peraluminous	Basic
	SL11	49.51	4.97	14.69	**15.35**	Peraluminous	Basic
Granulite	SL4	64.49	7.15	12.23	**14.76**	Peraluminous	Intermediate
	SL13	65.21	7.67	10.99	**13.83**	Peraluminous	Intermediate
Mafic granulite	SL5	43.28	3.76	**14.21**	13.33	*Metaluminous*	*Ultrabasic*
Felsic granulite	SL17	70.72	10.41	11.97	**13.37**	Peraluminous	Acidic

Criteria for chemical classification

Silica Saturation (SiO_2 Content)

- Ultrabasic (<45%)

- Basic (45-52%)

- Intermediate (52-66%)

- Acidic (>66%)

Alumina Saturation (Al_2O_3 Content)

-Peraluminous: Al_2O_3> (Na_2O+K_2O+CaO)

-Metaluminous: Al_2O_3< (Na_2O+K_2O+CaO) but Al_2O_3> (Na_2O+K_2O)

-Peralkaline: Al_2O_3< (Na_2O+K_2O)

In addition, Harker variations plotting of SiO_2 versus other oxides show some interesting trends (Figure 3.8). TiO_2, Fe_2O_3, MnO, MgO, CaO and P_2O_5 are decreasing against increasing of SiO_2 content. On the other hand, Al_2O_3 and Na_2O range in narrow ranges, about 15% and 3.5 %, respectively, that seems to be independent to SiO_2. Except samples SL1 and SL10, garnet gneiss, Na_2O are lower than those of the other rocks. Variation diagrams plotting between major oxides against Mg number *[Mg# = MgO/(FeO+MgO)]* are also interesting (Figure 3.9). Most of oxides seem to be independent to Mg#; however, SiO_2 and K_2O appear to decrease when Mg# increase.

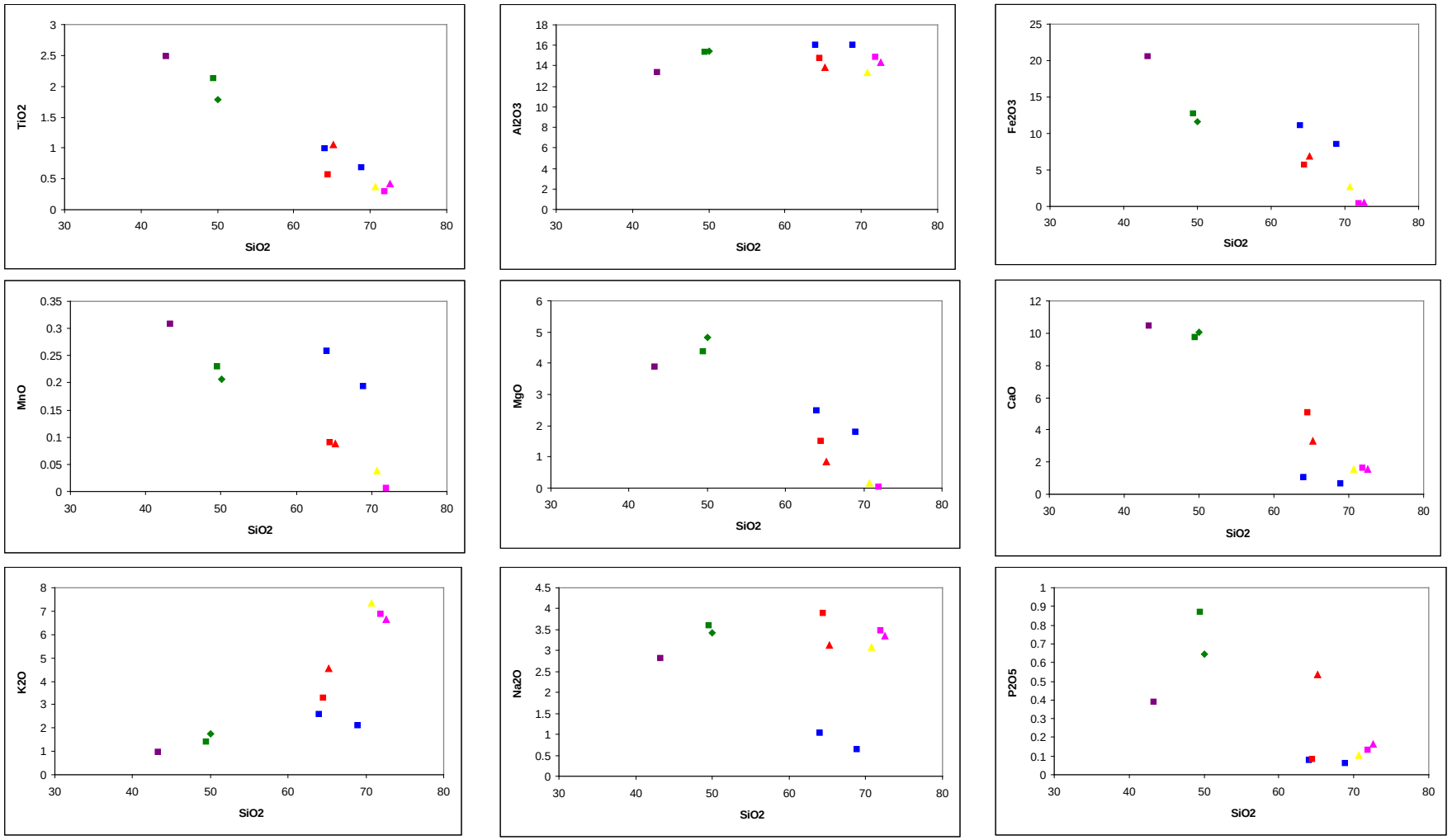

Figure 3.8 Harker variation diagrams plotting between SiO_2 against other oxides.

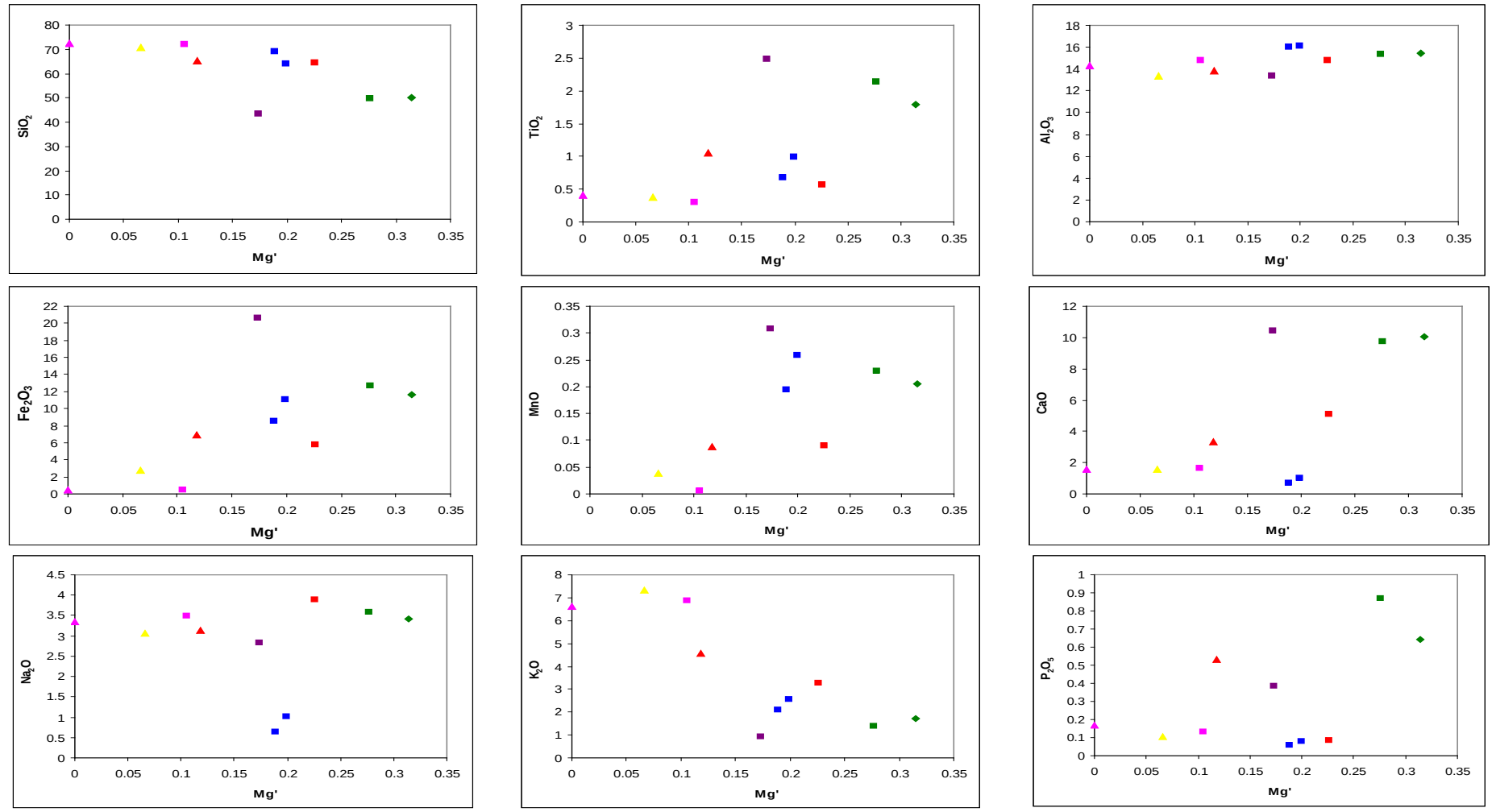

Figure 3.9 Variation diagrams plotting between Mg number (Mg#) versus major oxides [Mg#=MgO/(FeO+MgO)].

3.4 Mineral Chemistry

Electron Probe Micro-Analyzer (EPMA) (JEOL model JXA-8100) was used for investigation of mineral chemistry of 10 kinds of mineral significantly found in rock samples. About 3-5 spots were chosen for each mineral in each sample for analysis. These minerals are garnet, alkali feldspar, plagioclase, hornblende pyroxene, mica, sillimanite, rutile and ilmenite. The analytical results are summarized in Table 3.3; besides all data are collected in Appendix A. Details of each mineral is reported below.

Garnet: was found in samples of garnet gneiss, granulite, mafic granulite and graphitic gneiss. Most garnets are similarly characterized by pyralspite series which the main cation occupying X site is Fe indicating main composition of almandine garnet. However, their proportions are slightly different. Based on 12(O) formula, the average for almandine garnet in garnet gneiss is $[Fe_{0.70}Mg_{0.27}Mn_{0.03}]_3Al_2(SiO_4)_3$ whereas those averages in graphitic gneiss, granulite and mafic granulite are $[Fe_{0.86}Mg_{0.13}Mn_{0.01}]_3Al_2(SiO_4)_3$, $[Fe_{0.55}Mg_{0.44}Mn_{0.01}]_3Al_2(SiO_4)_3$ and $[Fe_{0.77}Mg_{0.23}Mn_{0.00}]_3Al_2(SiO_4)_3$, respectively.

Pyroxene: was found in granulite, mafic granulite and felsic granulite samples. These pyroxenes are characterized by orthopyroxene and clinopyroxene. The quadratic Ca-Mg-Fe pyroxene plot shows their composition proportion as in Figure 3.10. Based on 6(O) formula, average compositions of orthopyroxene in granulite, mafic granulite and felsic granulite are $[Ca_{0.02}Mg_{0.44}Fe_{0.54}]_2Si_2O_6$, $[Ca_{0.02}Mg_{0.38}Fe_{0.60}]_2Si_2O_6$ and $[Ca_{0.02}Mg_{0.20}Fe_{0.78}]_2Si_2O_6$, respectively. On the other hand, average compositions of clinopyroxene in granulite, mafic granulite and felsic granulite are $[Ca_{0.46}Mg_{0.32}Fe_{0.22}]_2Si_2O_6$, $[Ca_{0.46}Mg_{0.28}Fe_{0.26}]_2Si_2O_6$ and $[Ca_{0.44}Mg_{0.17}Fe_{0.39}]_2Si_2O_6$, respectively.

Amphibole: was only found in hornblende-biotite gneiss and a few grains in granulite. These amphiboles are dominated by Ca, Mg, Fe^{2+} and Al components which are compatible to hornblende range. Based on 23(O) formula, their average compositions was are $[Ca_{0.30}Fe_{0.30}Mg_{0.40}]_7(Al,Si)_8O_{22}(OH)_2$ and $[Ca_{0.30}Fe_{0.39}Mg_{0.31}]_7(Al,Si)_8O_{22}(OH)_2$ for hornblende-biotite gneiss and granulite, respectively.

Mica: was found in most gneissic rocks including garnet gneiss, graphitic gneiss and hornblende-biotite gneiss. Hornblende-biotite gneiss, in particular, shows orientation of biotite and hornblende. According to EPMA analyses, these micas can be divided into 2 groups, i.e., Mg rich and Fe rich compositions. Consequently, they are appropriated to be classed as

phlogopite and biotite for Mg and Fe micas, respectively. Phlogopite was found only in garnet gneiss. Based on 11(O) formula, the phlogopite contains a wide range of 0.498-0.850 K, 0.499-0.616 Fe^{2+} and 1.879-1.912 Mg. Regarding to biotite, they fall within the same range of about 0.158-0.937 K, 1.035-1.625 Fe^{2+} and 0.879-1.356 Mg.

Feldspar: was found in all of rock sample types but they vary in proportion and composition. Ternary feldspar componants, as represented by K, Na and Ca atomic proportion which K-Na-Ca triangular diagram plotting to represent three compositions of $KAlSi_3O_8$, $NaAlSi_3O_8$ and $CaAl_2Si_2O_8$ was taken for further interpretation, particularly estimation of the lowest temperature of feldspar crystallization at specific pressure (Figure 3.11). As a result, equilibrated temperatures of two feldspars coexisting in these rocks are mostly lower than 650 ºC. Moreover, perthitic feldspars in some samples also yield compatible temperature of exsolution between $KAlSi_3O_8$ and $NaAlSi_3O_8$ components (Figure 3.12) at lower than 445-515 ºC. The chemical compositions of feldspar vary in different rock types which are summarized in Table 3.4.

Other Minerals: including sillimanite, rutile and ilmenite were found in some particular rock samples. Sillimanite and rutile were found in garnet gneiss whereas ilmenite can be found in all sample groups except garnet gneiss. Although, some analytical results of these mineral are not good quality, these minerals seem to fall within the common composition of each mineral.

Table 3.3 Representative EPMA analyses of each mineral found in different rock types.

	Garnet				Alkali feldspar				Plagioclase					Orthopyroxene			Clinopyroxene		
	Garnet Gneiss	Graphitic Gneiss	Granulite	Mafic Granulite	Garnet Gneiss	Graphitic Gneiss	Granulite	Felsic Granulite	Garnet Gneiss	Graphitic Gneiss	Hornblende-Biotite Gneiss	Granulite	Mafic Granulite	Granulite	Mafic Granulite	Felsic Granulite	Granulite	Mafic Granulite	Felsic Granulite
Comment	SL1_grt	SL6_grt	SL4_grt	SL5_grt	SL1_K-fel	SL1_K-fel	SL13_K-fel	SL17_K-fel	SL1_Pl	SL1_Pl	SL11_Pl	SL4_Pl	SL5_Pl	SL4_opx	SL5_opx	SL17_opx	SL4_cpx	SL5_cpx	SL17_cpx
SiO_2	38.67	36.95	37.79	37.61	62.68	36.35	64.70	63.16	52.60	60.30	58.71	57.51	56.44	50.20	47.38	46.82	50.55	49.81	47.57
TiO_2	0.00	0.09	0.09	0.12	0.05	0.00	0.00	0.03	0.00	0.01	0.00	0.01	0.00	0.13	0.04	0.15	0.24	0.22	0.17
Al_2O_3	22.35	21.40	21.66	20.92	20.12	18.14	18.97	18.48	20.22	23.72	24.84	25.72	26.40	0.66	0.90	0.24	1.64	2.09	0.84
Cr_2O_3	0.02	0.00	0.00	0.03	0.00	0.00	0.00	0.01	0.00	0.00	0.02	0.00	0.02	0.01	0.00	0.00	0.00	0.03	0.00
FeO (Total)	22.18	32.74	27.61	30.69	0.01	0.03	0.02	0.03	0.01	0.09	0.15	0.35	0.08	32.52	35.77	44.70	13.29	16.63	26.20
MnO	1.53	0.87	0.07	0.08	0.00	0.00	0.01	0.00	0.00	0.00	0.00	0.00	0.01	0.02	0.08	0.67	0.01	0.01	0.27
MgO	9.37	2.38	4.60	3.29	0.00	0.00	0.00	0.00	0.01	0.07	0.00	0.00	0.00	14.54	12.11	6.16	10.53	9.02	5.28
ZnO	0.09	0.01	0.00	0.00	0.00	0.00	0.00	0.00	0.00	0.00	0.01	0.00	0.06	0.06	0.06	0.15	0.10	0.13	0.12
CaO	5.28	6.31	6.53	6.89	0.25	0.15	0.19	0.10	5.36	4.94	6.92	7.22	8.79	0.92	0.70	1.07	21.06	21.24	18.08
Na_2O	0.02	0.01	0.02	0.01	3.41	2.09	2.31	1.73	7.43	8.71	6.21	6.95	6.17	0.00	0.01	0.02	0.40	0.40	0.37
K_2O	0.02	0.01	0.00	0.00	12.95	8.74	11.19	13.76	0.00	0.13	0.43	0.00	0.01	0.01	0.00	0.00	0.00	0.00	0.01
Total	99.52	100.80	98.43	99.66	99.49	92.50	97.40	97.29	85.66	97.99	97.29	97.76	98.02	99.06	97.09	99.97	97.83	99.59	98.95
Formula	12 (O)				8 (O)				8 (O)					6 (O)			6 (O)		
Si	2.996	2.950	3.003	3.000	2.901	3.043	3.000	2.979	2.734	2.733	2.681	2.625	2.579	1.986	1.957	1.969	1.967	1.937	1.945
Ti	0.000	0.005	0.005	0.007	0.002	0.000	0.000	0.001	0.000	0.000	0.000	0.000	0.000	0.004	0.001	0.005	0.007	0.006	0.005
Al	2.020	2.014	2.028	1.967	1.098	1.027	1.036	1.027	1.239	1.267	1.337	1.383	1.422	0.031	0.044	0.012	0.075	0.096	0.041
Cr	0.001	0.000	0.000	0.002	0.000	0.000	0.000	0.000	0.000	0.000	0.001	0.000	0.001	0.000	0.000	0.000	0.000	0.001	0.000
Fe^{3+}	0.076	0.115	0.000	0.027	0.000	0.001	0.001	0.001	0.001	0.003	0.006	0.014	0.003	0.000	0.060	0.064	0.010	0.069	0.129
Fe^{2+}	1.347	2.071	1.834	2.020	-	-	-	-	-	-	-	-	-	1.076	1.176	1.508	0.423	0.472	0.767
Mn	0.100	0.059	0.005	0.006	0.000	0.000	0.000	0.000	0.000	0.000	0.000	0.000	0.001	0.001	0.003	0.024	0.000	0.000	0.009
Mg	1.072	0.283	0.545	0.391	0.000	0.000	0.000	0.000	0.001	0.005	0.000	0.000	0.000	0.858	0.746	0.386	0.611	0.523	0.322
Zn	0.005	0.000	0.000	0.000	0.000	0.000	0.000	0.000	0.000	0.000	0.000	0.000	0.002	0.002	0.002	0.005	0.003	0.004	0.004
Ca	0.434	0.539	0.556	0.589	0.012	0.008	0.010	0.005	0.298	0.240	0.338	0.353	0.430	0.039	0.031	0.048	0.878	0.885	0.792
Na	0.003	0.001	0.002	0.001	0.306	0.194	0.208	0.158	0.749	0.765	0.550	0.615	0.546	0.000	0.001	0.001	0.030	0.030	0.029
K	0.002	0.001	0.000	0.000	0.764	0.535	0.662	0.828	0.000	0.007	0.025	0.000	0.000	0.001	0.000	0.000	0.000	0.000	0.000
Total*	8.025	8.039	7.979	8.009	5.084	4.809	4.917	5.000	5.021	5.020	4.937	4.990	4.984	3.996	4.020	4.021	4.003	4.023	4.044

Table 3.3 (cont.)

	Hornblende		Mica (Phlogopite and Biotite)				Sillimanite, Rutile and Ilmenite						
	Hornblende-Biotite Gneiss	Granulite	Garnet Gneiss	Graphitic Gneiss	Hornblende-Biotite Gneiss	Granulite	Garnet Gneiss		Graphitic Gneiss	Hornblende-Biotite Gneiss	Granulite	Mafic Granulite	Felsic Granulite
Comment	SL11_Hbl	SL4_Hbl	SL1_lep	SL6_lep	SL11_lep	SL4_lep	SL1_sil	SL1_rt	SL16_Iln	SL11_Iln	SL4_Iln	SL5_Iln	SL17_Iln
SiO_2	41.72	39.89	36.72	36.48	35.36	40.02	36.01	0.01	0.01	0.01	0.01	0.00	0.01
TiO_2	2.01	2.50	4.51	6.90	5.02	2.29	0.01	98.76	40.55	44.70	52.79	49.57	51.22
Al_2O_3	10.14	11.03	15.70	12.04	13.60	11.07	63.58	0.03	0.00	0.03	0.03	0.06	0.03
Cr_2O_3	0.05	0.10	0.05	0.00	0.07	0.02	0.08	0.10	0.03	0.08	0.11	0.00	0.05
FeO (Total)	13.62	17.97	9.90	25.02	15.86	22.16	0.12	0.07	36.01	45.68	45.29	49.57	47.98
MnO	0.34	0.01	0.01	0.02	0.10	0.13	0.00	0.00	0.09	1.35	0.01	0.00	0.35
MgO	10.32	8.15	17.24	8.25	11.30	7.92	0.00	0.00	0.23	0.25	0.78	0.63	0.25
ZnO	0.02	0.00	0.01	0.10	0.02	0.04	0.00	0.00	0.04	0.00	0.04	0.15	0.04
CaO	10.86	10.78	0.00	0.00	0.00	10.68	0.1	0.00	0.00	0.00	0.00	0.00	0.00
Na_2O	1.22	1.41	0.11	0.11	0.06	1.77	0.00	0.00	0.00	0.00	0.00	0.00	0.00
K_2O	1.31	0.02	8.96	5.66	9.04	1.67	0.01	0.00	0.01	0.00	0.00	0.00	0.00
Total	91.63	91.94	93.21	94.60	90.42	97.79	99.81	98.98	77.01	92.11	99.07	99.98	99.92
Formula	23 (O)		11 (O)				5 (O)	2 (O)	3 (O)				
Si	6.609	6.404	2.732	2.833	2.810	2.979	0.975	0.000	0.000	0.000	0.000	0.000	0.000
Ti	0.240	0.320	0.253	0.403	0.300	0.128	0.000	0.998	0.998	0.941	1.004	0.954	0.979
Al	1.893	2.087	1.377	1.102	1.274	0.971	2.029	0.000	0.000	0.001	0.001	0.002	0.001
Cr	0.006	0.012	0.003	0.000	0.005	0.001	0.002	0.001	0.001	0.002	0.002	0.000	0.001
Fe^{3+}	1.542	1.386	0.000	0.000	0.000	0.000	0.003	0.003	0.002	0.166	0.000	0.130	0.058
Fe^{2+}	0.262	1.026	0.616	1.625	1.054	1.380	-	0.000	0.984	0.904	0.957	0.931	0.963
Mn	0.046	0.001	0.000	0.001	0.007	0.008	0.000	0.000	0.003	0.032	0.000	0.000	0.008
Mg	2.438	1.951	1.912	0.955	1.339	0.879	0.000	0.000	0.011	0.010	0.029	0.024	0.009
Zn	0.003	0.000	0.000	0.006	0.001	0.002	0.000	0.000	0.001	0.000	0.001	0.003	0.001
Ca	1.843	1.854	0.000	0.000	0.000	0.852	0.000	0.000	0.000	0.000	0.000	0.000	0.000
Na	0.374	0.439	0.016	0.017	0.009	0.256	0.000	0.000	0.000	0.000	0.000	0.000	0.000
K	0.265	0.004	0.850	0.560	0.916	0.158	0.000	0.000	0.000	0.000	0.000	0.000	0.000
Total*	15.520	15.466	7.759	7.502	7.714	7.614	3.009	1.003	2.001	2.059	1.995	2.044	2.019

Table 3.4 Feldspar compositions in each rock type recalculated from data in Table 3.3.

sample	Plagioclase	K-feldspar
Garnet Gneiss	$[Ca_{0.26}Na_{0.73}K_{0.01}](AlSi)_4O_8$	$[K_{0.57}Na_{0.36}Ca_{0.07}](AlSi)_4O_8$
Graphitic Gneiss	$[Ca_{0.24}Na_{0.75}K_{0.01}](AlSi)_4O_8$	$[K_{0.73}Na_{0.26}Ca_{0.01}](AlSi)_4O_8$
Hornblende-Biotite Gneiss	$[Ca_{0.37}Na_{0.60}K_{0.03}](AlSi)_4O_8$	nd
Granulite	$[Ca_{0.34}Na_{0.65}K_{0.01}](AlSi)_4O_8$	$[K_{0.75}Na_{0.24}Ca_{0.01}](AlSi)_4O_8$
Mafic Granulite	$[Ca_{0.44}Na_{0.56}K_{0.00}](AlSi)_4O_8$	nd
Felsic Granulite	Nd	$[K_{0.84}Na_{0.16}Ca_{0.00}](AlSi)_4O_8$

nd: no detect

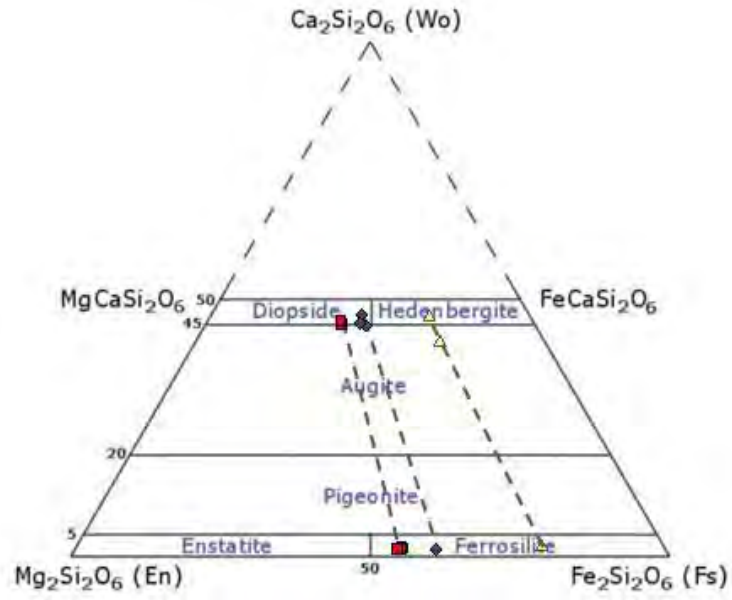

Granulite, Mafic Granulite, Felsic Granulite

Figure 3.10 Quadratic pyroxen plots show mineral chemistry of pyroxene in each sample (fields after Alden, 2009).

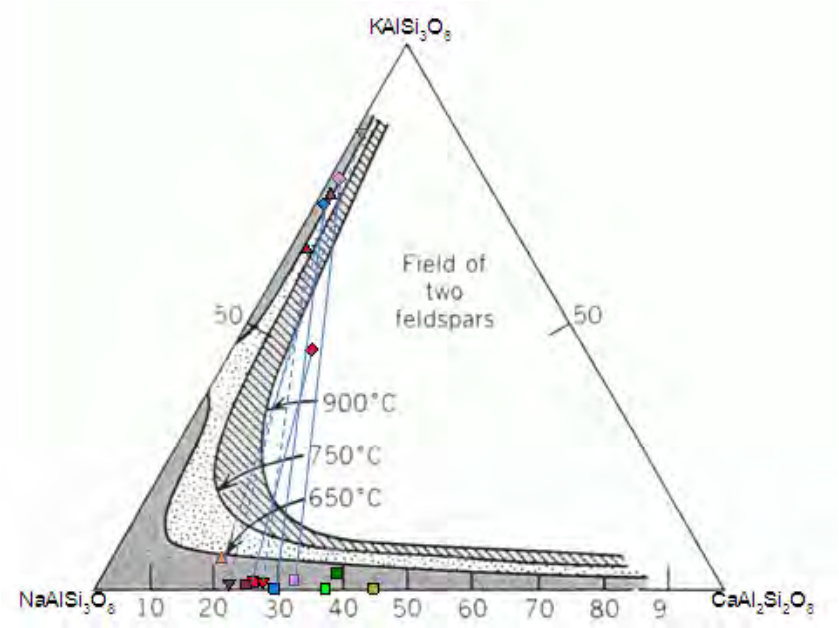

Figure 3.11 Ternary feldspar plot with isothermal lines at 1 kbar (after Ribbe, 1975) indicates mineral chemistry of alkali feldspar and coexisting plagioclase in each sample. Dash tied lines are connected between compositions of perthitic exsolutionand its alkali feldspar host. Solid tied lines are connected compositions of coexisting alkali feldspar and plagioclase in same rock sample.

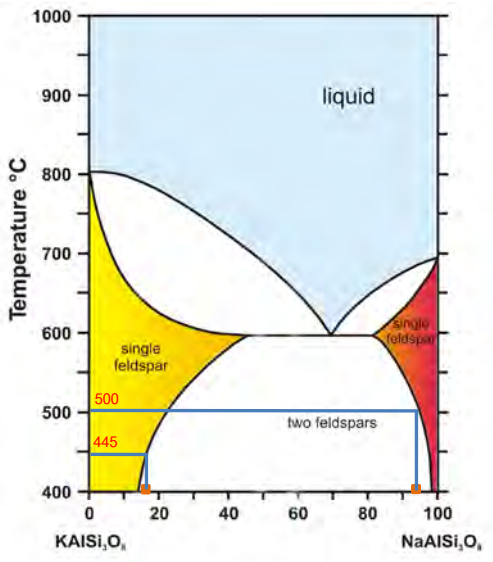

Figure 3.12 $KAlSi_3O_8$-$NaAlSi_3O_8$ binary system at 5 Kbar (from *the Science Education Resource Center at Carleton College (SECC)*, 2007) shows temperature ranging of lowest temperature for re-equilibration of exsolution perthitic feldspar sample SL17(felsic granulite).

CHAPTER IV

DISCUSSION, CONCLUSION AND RECOMMENDATION

CHAPTER IV

DISCUSSION, CONCLUSION AND RECOMMENDATION

4.1 Gem-Bearing Rocks

All of gem-related samples were collected from the Highland Complex (HC) of Sri Lanka. Based on their metamorphic and petrographic features, these rocks can be subdivided into 6 types including garnet gneiss, graphitic gneiss, hornblende-biotite gneiss, granulite, mafic granulite and felsic granulite. Their mineral assemblages are quite similar in all types that may lead to the same grade of metamorphism and similar chemical composition. The major minerals are mostly characterized by plagioclase, alkali feldspar, almandine garnet, clinopyroxene, orthopyroxene, hornblende and mica with the accessories of rutile, ilmenite and sillimanite. Petrographic description yields perthitic textures a common texture found in all rock types. Garnet gneiss contains almandine garnet formed as porphyroblast within groundmass of quartz and feldspar. Graphitic gneiss usually contains alkali feldspar and other minerals as matrix surrounding porphyroblasts of garnet. Biotite and opaque mineral (seem likely graphite) usually form lepidoblastic textures. Garnet was found as small size and less amount. Hornblende-biotite gneiss usually contains hornblende, biotite and plagioclase. Triple junction and mineral orientation are clearly observed. Granulite contains more mafic minerals such as pyroxene and hornblende which has appeared to have well developed triple junction. Mafic granulite usually presents large porphyroblasts of garnet and pyroxene whereas quartz and other minerals is matrix. Although garnets were found with higher amount in this rock type, its proportion is still less than those in garnet gneiss. Felsic granulite also contains pyroxene and alkali feldspar which the later shows clearly perthitic texture. In conclusion, these rock types are similarly characterized by mineral assemblages and petrographic feature. However, garnet gneiss appears to be the most significant gem-bearing rock based on its coarse-grained assemblage and more amount of garnet.

Regarding to whole-rock geochemistry, these rocks are high alumina saturation with various ranges of silica saturation. Most of them are peraluminous except mafic granulite fall in metaluminous and ultrabasic composition. For silica saturation, garnet gneiss is between acidic and intermediate whereas graphitic gneiss, granulite and hornblende-biotite gneiss are acidic, intermediate and basic compositions, respectively. Besides, felsic granulite seems to have

acidic composition. These various silica saturation may lead to different gem formation that have been found in particular areas such as aquamarine, tourmaline, garnet, moonstone, zircon, corundum, etc.

4.2 Metamorphism

Most of selected rocks show well developed triple junction and have some index minerals such as sillimanite, pyroxene and garnet that can indicate high temperature and pressure of forming. ACF triangular diagram as present in Figure 4.1 is plotted to investigate and reconstruct the appropriate protoliths of these rock.

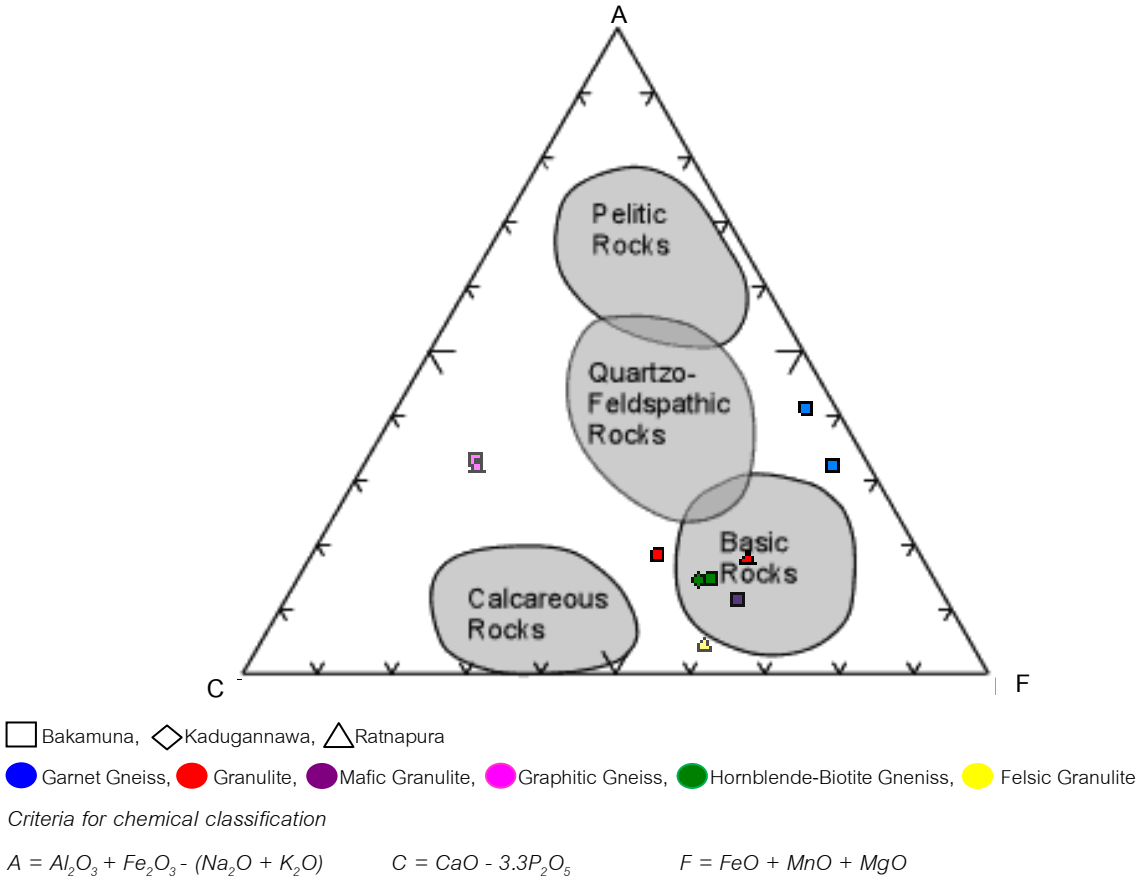

Figure 4.1 ACF diagram showing three groups of rock samples falling in different fields of protolith.

From ACF diagram (Figure 4.1), the rock samples can be subdivided into 3 groups. The first group falls within basic rocks composition including granulite, felsic granulite, mafic granulite and hornblende-biotite gneiss. They are mostly agreeable to petrographic investigation except felsic granulite should fall in the other fields because their essential minerals are significantly characterized by felsic minerals such as alkali feldspar and quartz.

However, pyroxene is also distinguished that would be main source of FeO, MgO and MnO yielding such result.

The second group, garnet gneiss, has unusually low CaO composition but it closes to quartzo-feldspathic protolith. The last group, graphitic gneiss, falls out completely from the common protolith fields.

For mineral chemistry, the results of pyroxene and feldspar groups were focused to understand chemical composition of mineral and P-T condition of crystallization. Figure 3.10 shows chemical composition of clinopyroxene and orthopyroxene that can be used to classify these pyroxenes. Orthopyroxene is mostly classified as ferosilite composition whereas clinopyroxene varies between diopside and hedenbergite areas.

Feldspar group, plagioclase and alkali feldspar, are also used to interpret and predict the temperature of crystallization. Plagioclase and alkali feldspar, which growth together in same sample, are used to correlate the relationship in ternary feldspar plot between $KAlSi_3O_8$, $NaAlSi_3O_8$ and $CaAl_2Si_2O_8$ (Figure 3.11). Moreover, perthitic composition is also plotted (Figure 3.12). Most of composition of feldspar falls within the field of temperature lower than 650 ºC. This result represents the equilibrium temperature of coexisting two feldspars equal or lower than 650 ºC. Binary component phase of solid-solution feldspar shows the lowest temperature (445 -500 ºC) of re-equilibrium (exsolution) of perthitic feldspar. These are good agreement of subsolidus re-equilibration of the system or retrograde metamorphism after reaching the peak metamorphism (granulite facies) above such temperatures reported.

4.3 Recommendations

Due to limited of time under this study some EPMA analyses have low quality which may be caused by polish-thin sectioning and perhaps coating process. Other significant elements need to be analyzed. Subsequently, the estimation of pressure and temperature condition might be improved and yielding more accurate result.

In addition, for gem exploration in Sri Lanka especially in Highland Complex (HC), the most interesting and heist potential rock type should be garnet gneiss. They have highest amount of gem with bigger gem.

References

Dissanayake C.B., R. Chandrajith R. and Tobschall H.J. 2000. The geology, mineralogy and rare element geochemistry of the gem deposits of Sri Lanka. Bulletin of the Geological Society of Finland. 72, Parts 1–2, 5–20.

Fernando, G.W.A.R., Attanyake, A.N.B. and Hofmeister, W. 2005. Corundum-spinel-taafeite-scheelite bearing metasomatites in Bakamuna, Srilanka: modeling of its formation. Proceedings of the International Symposium on Gem-Material and Modern Analytical Methods, Hanoi, 117-127.

Katz. M.B. 2000. Sri Lanka-India intraplate tectonics-Precambrian to Present. Gondwana Research, 3(1): 3-5.

Mathavan, V., Prame, W.K.B.N. and Cooray, P.G. 1998. Geology of the high grade Proterozoic terrains of Sri Lanka and the assembly of Gondwana: An update on recent developments. Gondwana Research, 2(2): 237-250.

Osanai, Y., Sajeev, K., Owada, M., Kehelpannala, K.V.W., Prame, W.K.B., Nakano, N. and Jayatileke, S. 2006. Metamorphic evolution of high-pressure and ultrahigh-temperature granulites from the Highland Complex, Sri Lanka. Journal of Asian Earth Sciences, 28: 20-37.

Tennakoon, S., Rupasinge, M. and Dissanayake C.B. 2005. New in-situ and elluvial corundum deposits around Wellawaya area, Sri Lanka. Proceedings of the International Symposium on Gem-Material and Modern Analytical Methods, Hanoi, 241-250.

Wilson, T.J., Gunow, A.M. and Hanson, R.E. 1997. Gondwana assembly: The view from southern Africa and East Gondwana. Journal of Geodynamics, 23(314): 263-286.

APPENDIX

MINERAL CHEMISTRY ANALYSIS

	Orthopyroxene							Clinopyroxene						
	Granulite				Mafic Granulite	Felsic Grnulite		Granulite		Mafic Granulite			Felsic Grnulite	
Comment	SL4_Opx	SL4_Opx	SL4_Opx	SL4_Opx	SL5_Opx	SL17_Opx	SL17_Opx	SL4_Cpx	SL4_Cpx	SL5_Cpx	SL5_Cpx	SL5_Cpx	SL17_Cpx	SL17_Cpx
SiO_2	50.20	50.31	49.68	49.87	47.38	46.87	46.82	50.67	50.55	49.64	49.81	49.60	48.27	47.57
TiO_2	0.13	0.11	0.19	0.17	0.04	0.17	0.15	0.23	0.24	0.17	0.22	0.22	0.15	0.17
Al_2O_3	0.66	0.58	0.94	0.65	0.90	0.26	0.24	1.48	1.64	1.92	2.09	1.95	0.79	0.84
Cr_2O_3	0.01	0.06	0.04	0.00	0.00	0.04	0.00	0.00	0.00	0.01	0.03	0.01	0.05	0.00
FeO (Total)	32.52	32.02	31.38	31.61	35.77	44.55	44.70	13.45	13.29	17.88	16.63	17.44	23.11	26.20
MnO	0.02	0.00	0.02	0.05	0.08	0.43	0.67	0.02	0.01	0.03	0.01	0.05	0.22	0.27
MgO	14.54	14.48	14.56	14.72	12.11	6.21	6.16	10.60	10.53	9.03	9.02	9.31	5.17	5.28
ZnO	0.06	0.13	0.09	0.01	0.06	0.18	0.15	0.10	0.10	0.07	0.13	0.12	0.04	0.12
CaO	0.92	0.85	0.76	0.84	0.70	1.11	1.07	20.88	21.06	20.30	21.24	20.50	20.43	18.08
Na_2O	0.00	0.00	0.02	0.03	0.01	0.00	0.02	0.37	0.40	0.39	0.40	0.37	0.42	0.37
K_2O	0.01	0.01	0.00	0.01	0.00	0.00	0.00	0.00	0.00	0.00	0.00	0.01	0.00	0.01
Total	99.06	98.55	97.69	97.98	97.09	99.82	99.97	97.79	97.83	99.44	99.59	99.62	98.65	98.95
Formula 6(O)														
Si	1.986	1.996	1.984	1.988	1.957	1.971	1.969	1.972	1.967	1.940	1.937	1.934	1.960	1.945
Ti	0.004	0.003	0.006	0.005	0.001	0.006	0.005	0.007	0.007	0.005	0.006	0.006	0.004	0.005
Al	0.031	0.027	0.044	0.031	0.044	0.013	0.012	0.068	0.075	0.088	0.096	0.089	0.038	0.041
Cr	0.000	0.002	0.001	0.000	0.000	0.001	0.000	0.000	0.000	0.000	0.001	0.000	0.002	0.000
Fe^{3+}	0.000	0.000	0.000	0.000	0.060	0.000	0.000	0.000	0.000	0.000	0.000	0.000	0.000	0.000
Fe^{2+}	1.076	1.062	1.048	1.054	1.236	1.566	1.572	0.438	0.432	0.584	0.541	0.596	0.785	0.896
Mn	0.001	0.000	0.001	0.002	0.003	0.015	0.024	0.001	0.000	0.001	0.000	0.002	0.007	0.009
Mg	0.858	0.856	0.867	0.875	0.746	0.389	0.386	0.615	0.611	0.526	0.523	0.541	0.313	0.322
Zn	0.002	0.004	0.003	0.000	0.002	0.006	0.005	0.003	0.003	0.002	0.004	0.003	0.001	0.004
Ca	0.039	0.036	0.033	0.036	0.031	0.050	0.048	0.871	0.878	0.850	0.885	0.856	0.889	0.792
Na	0.000	0.000	0.001	0.003	0.001	0.000	0.001	0.028	0.030	0.030	0.030	0.028	0.033	0.029
K	0.001	0.000	0.000	0.000	0.000	0.000	0.000	0.000	0.000	0.000	0.000	0.000	0.000	0.000
Total*	3.996	3.987	3.998	3.993	4.020	4.017	4.021	4.001	4.003	4.026	4.023	4.029	4.032	4.044
Atomic %														
Ca	1.98	1.86	1.68	1.83	1.53	2.49	2.39	45.27	45.69	43.36	45.41	43.55	44.73	39.40
Fe^{2+}	54.53	54.34	53.81	53.63	61.40	78.11	78.35	22.76	22.51	29.81	27.75	28.92	39.51	44.58
Mg	43.48	43.81	44.52	44.54	37.06	19.41	19.26	31.97	31.80	26.83	26.84	27.53	15.76	16.02

Table 1: Representative EPMA analysis of pyroxene was found in different rock types.

	Hornblende						Mica (Phlogopite and Biotite)								Garnet					
	Hornblende-biotite gneiss					Granulite	Garnet gneiss			Graphitic gneiss	Granulite	Hornblende-biotite gneiss			Garnet gneiss		Granulite	Mafic granulite	Graphitic gneiss	
Comment	SL11_hbl	SL11_hbl	SL11_hbl	SL11_hbl	SL11_hbl	SL4_hbl	SL1_leb	SL1_leb	SL10_leb	SL6_leb	SL13_leb	SL11_leb	SL11_leb	SL11_leb	SL1_grt	SL10_grt	SL4_grt	SL5_grt	SL6_grt	SL16_grt
SiO_2	41.72	41.04	41.35	41.07	41.38	39.89	40.542	36.72	33.82	36.48	40.02	35.29	35.28	35.36	38.67	38.76	37.79	37.61	36.95	33.49
TiO_2	2.01	1.92	1.98	1.96	2.03	2.50	3.85	4.51	4.40	6.90	2.29	4.88	4.94	5.02	0.00	0.03	0.09	0.12	0.09	0.00
Al_2O_3	10.14	10.27	10.20	10.41	10.16	11.03	14.616	15.70	14.30	12.04	11.07	13.64	13.64	13.60	22.35	22.28	21.66	20.92	21.40	18.78
Cr_2O_3	0.05	0.02	0.03	0.07	0.00	0.10	0.119	0.05	0.04	0.00	0.02	0.04	0.03	0.07	0.02	0.02	0.00	0.03	0.00	0.03
FeO	13.62	14.12	13.75	14.17	13.86	17.97	8.072	9.90	7.86	25.02	22.16	15.59	15.53	15.86	22.18	25.08	27.61	30.69	32.74	22.79
MnO	0.34	0.23	0.33	0.33	0.32	0.01	0.017	0.01	0.02	0.02	0.13	0.17	0.15	0.10	1.53	0.41	0.07	0.08	0.87	0.76
MgO	10.32	10.15	10.29	10.36	10.31	8.15	17.155	17.24	15.41	8.25	7.92	11.42	11.36	11.30	9.37	10.93	4.60	3.29	2.38	2.03
ZnO	0.02	0.05	0.21	0.08	0.00	0.00	0.12	0.01	0.09	0.10	0.04	0.07	0.01	0.02	0.09	0.00	0.00	0.00	0.01	0.00
CaO	10.86	10.85	10.78	10.78	10.76	10.78	0	0.00	0.00	0.00	10.68	0.00	0.00	0.00	5.28	1.35	6.53	6.89	6.31	4.39
Na_2O	1.22	1.25	1.26	1.30	1.28	1.41	0.184	0.11	0.14	0.11	1.77	0.06	0.03	0.06	0.02	0.00	0.02	0.01	0.01	0.00
K_2O	1.31	1.32	1.36	1.35	1.34	0.02	5.279	8.96	8.06	5.66	1.67	9.05	9.13	9.04	0.02	0.00	0.00	0.00	0.01	0.00
Total	91.63	91.24	91.56	91.89	91.44	91.94	89.95	93.21	84.20	94.60	97.79	90.21	90.10	90.42	99.52	98.89	98.43	99.66	100.80	93.66
Formula	23 (O)						11 (O)								12 (O)					
Si	6.609	6.555	6.575	6.519	6.581	6.404	3.00	2.732	2.767	2.833	2.979	2.809	2.812	2.810	2.966	2.981	3.003	3.000	2.950	3.149
Ti	0.240	0.231	0.237	0.235	0.243	0.302	0.21	0.253	0.271	0.403	0.128	0.292	0.296	0.300	0.000	0.002	0.005	0.007	0.005	0.000
Al	1.893	1.933	1.911	1.948	1.905	2.087	1.27	1.377	1.378	1.102	0.971	1.280	1.281	1.274	2.020	2.019	2.028	1.967	2.014	2.081
Cr	0.006	0.002	0.004	0.009	0.000	0.012	0.01	0.003	0.003	0.000	0.001	0.002	0.002	0.005	0.001	0.001	0.000	0.002	0.000	0.002
Fe^{3+}	1.542	1.695	1.662	1.781	1.646	1.386	0.00	0.000	0.000	0.000	0.000	0.000	0.000	0.000	0.076	0.022	0.000	0.027	0.115	0.000
Fe^{2+}	0.262	0.191	0.166	0.100	0.197	1.026	0.50	0.616	0.538	1.625	1.380	1.038	1.035	1.054	1.347	1.591	1.834	2.020	2.071	2.376
Mn	0.046	0.031	0.045	0.044	0.043	0.001	0.00	0.000	0.001	0.001	0.008	0.011	0.010	0.007	0.100	0.027	0.005	0.006	0.059	0.060
Mg	2.438	2.418	2.439	2.453	2.443	1.951	1.89	1.912	1.879	0.955	0.879	1.356	1.349	1.339	1.072	1.253	0.545	0.391	0.283	0.284
Zn	0.003	0.006	0.025	0.009	0.000	0.000	0.01	0.000	0.005	0.006	0.002	0.004	0.001	0.001	0.005	0.000	0.000	0.000	0.000	0.000
Ca	1.843	1.857	1.837	1.834	1.833	1.854	0.00	0.000	0.000	0.000	0.852	0.000	0.000	0.000	0.434	0.112	0.556	0.589	0.539	0.442
Na	0.374	0.387	0.388	0.399	0.394	0.439	0.03	0.016	0.022	0.017	0.256	0.009	0.005	0.009	0.003	0.000	0.002	0.001	0.001	0.000
K	0.265	0.268	0.275	0.273	0.271	0.004	0.50	0.850	0.841	0.560	0.158	0.920	0.928	0.916	0.002	0.000	0.000	0.000	0.001	0.000
Total*	15.520	15.574	15.562	15.604	15.557	15.466	7.41	7.759	7.704	7.502	7.614	7.721	7.717	7.714	8.025	8.007	7.979	8.009	8.039	7.810
Atomic %																				
Fe^{2+}	29.66	30.61	29.94	30.50	30.12	38.79								Mg	42.57	43.66	22.86	16.17	11.74	10.44
Mg	40.06	39.25	39.96	39.77	39.92	31.38								Fe^{2+}	53.47	55.41	76.95	83.60	85.82	87.35
Ca	30.28	30.15	30.10	29.74	29.96	29.83								Mn	3.96	0.93	0.19	0.23	2.44	2.21

Table 2: Representative EPMA analyses of hornblende, mica and garnet were found in different rock types.

	Plagioclase							Alkali feldspar				Perthite and K-feldspar host				
	Garnet gneiss		Granulite		Mafic granulite	Graphitic gneiss	Hornblende-biotite gneiss	Garnet gneiss		Graphitic gneiss	Granulite	Garnet gneiss		Graphitic gneiss	Felsic garnulite	
Comment	SL1_pl	SL10_pl	SL4_pl	SL13_pl	SL5_pl	SL6_pl	SL11_pl	SL1_K-fel	SL10_K-fel	SL6_K_h	SL13_K-fel	SL10_pth	SL10_host	SL6_pth	SL17_host	SL17_pth
SiO_2	52.60	49.60	57.51	59.43	56.44	60.30	58.71	62.68	59.74	63.35	64.70	54.64	55.38	60.87	63.16	63.14
TiO_2	0.00	0.00	0.01	0.02	0.00	0.01	0.00	0.05	0.08	0.00	0.00	0.00	0.01	0.03	0.03	0.03
Al_2O_3	20.22	20.74	25.72	25.16	26.40	23.72	24.84	20.12	17.60	18.14	18.97	21.21	17.34	23.11	18.48	22.00
Cr_2O_3	0.00	0.00	0.00	0.01	0.02	0.00	0.02	0.00	0.00	0.00	0.00	0.00	0.03	0.00	0.01	0.00
FeO	0.01	0.00	0.35	0.05	0.08	0.09	0.15	0.01	0.00	0.03	0.02	0.02	0.05	0.14	0.03	0.02
MnO	0.00	0.03	0.00	0.00	0.01	0.00	0.00	0.00	0.00	0.00	0.01	0.00	0.00	0.02	0.00	0.00
MgO	0.01	0.00	0.00	0.00	0.00	0.07	0.00	0.00	0.00	0.00	0.00	0.00	0.00	0.00	0.00	0.00
ZnO	0.00	0.00	0.00	0.00	0.06	0.00	0.01	0.00	0.03	0.00	0.00	0.02	0.00	0.04	0.00	0.01
CaO	5.36	4.44	7.22	6.46	8.79	4.94	6.92	0.25	2.34	0.15	0.19	5.09	0.28	4.48	0.10	3.44
Na_2O	7.43	7.50	6.95	7.84	6.17	8.71	6.21	3.41	4.51	2.09	2.31	7.82	2.39	9.24	1.73	8.52
K_2O	0.00	0.19	0.00	0.23	0.01	0.13	0.43	12.95	6.88	8.74	11.19	0.14	6.48	0.10	13.76	0.95
Total	85.66	82.51	97.76	99.20	98.02	97.99	97.29	99.49	91.18	92.50	97.40	88.99	82.01	98.02	97.29	98.14
Formula 8(O)																
Si	2.734	2.680	2.625	2.670	2.579	2.733	2.681	2.901	2.950	3.043	3.000	2.733	2.988	2.757	2.979	2.841
Ti	0.000	0.000	0.000	0.001	0.000	0.000	0.000	0.002	0.003	0.000	0.000	0.000	0.001	0.001	0.001	0.001
Al	1.239	1.321	1.383	1.332	1.422	1.267	1.337	1.098	1.025	1.027	1.036	1.250	1.103	1.234	1.027	1.166
Cr	0.000	0.000	0.000	0.000	0.001	0.000	0.001	0.000	0.000	0.000	0.000	0.000	0.001	0.000	0.000	0.000
Fe^{3+}	0.001	0.000	0.014	0.002	0.003	0.003	0.006	0.000	0.000	0.001	0.001	0.001	0.002	0.005	0.001	0.001
Fe^{2+}	-	-	-	-	-	-	-	-	-	-	-	-	-	-	-	-
Mn	0.000	0.001	0.000	0.000	0.001	0.000	0.000	0.000	0.000	0.000	0.000	0.000	0.000	0.001	0.000	0.000
Mg	0.001	0.000	0.000	0.000	0.000	0.005	0.000	0.000	0.000	0.000	0.000	0.000	0.000	0.000	0.000	0.000
Zn	0.000	0.000	0.000	0.000	0.002	0.000	0.000	0.000	0.001	0.000	0.000	0.001	0.000	0.001	0.000	0.000
Ca	0.298	0.257	0.353	0.311	0.430	0.240	0.338	0.012	0.124	0.008	0.010	0.273	0.016	0.217	0.005	0.166
Na	0.749	0.786	0.615	0.683	0.546	0.765	0.550	0.306	0.432	0.194	0.208	0.758	0.250	0.811	0.158	0.743
K	0.000	0.013	0.000	0.013	0.000	0.007	0.025	0.764	0.433	0.535	0.662	0.009	0.446	0.006	0.828	0.055
Total*	5.021	5.059	4.990	5.012	4.984	5.020	4.937	5.084	4.967	4.809	4.917	5.025	4.807	5.033	5.000	4.974
Atomic %																
Ca	28.48	24.34	36.49	30.88	44.05	23.69	37.06	1.14	12.52	1.03	1.08	26.23	2.29	21.01	0.50	17.20
Na	71.50	74.41	63.50	67.79	55.90	75.58	60.20	28.28	43.65	26.36	23.65	72.89	35.10	78.44	15.95	77.14
K	0.01	1.25	0.01	1.33	0.05	0.73	2.74	70.57	43.83	72.61	75.26	0.88	62.61	0.55	83.54	5.66

Table 3: Representative EPMA analyses of plagioclase and alkali feldspar, include perthite, were found in different rock types.

	Sillimamite		Rutile			Ilmenite							
	Garnet gneiss		Garnet gneiss			Granulite		Mafic granulite	Hornblende-biotite gneiss		Graphitic gneiss	Felsic garnulite	
Comment	SL1_sil_	SL10_sil	SL1_rtl	SL1_rtl	SL10_rtl	SL4_Iln	SL13_Iln	SL5_Iln	SL11_Iln	SL11_Iln	SL16_Iln	SL17_Iln	SL17_Iln
SiO_2	36.01	35.46	0.01	0.00	0.00	0.01	0.00	0.00	0.01	0.01	0.01	0.00	0.01
TiO_2	0.01	0.04	98.76	66.92	90.40	52.79	48.44	49.57	44.70	44.66	40.55	50.44	51.22
Al_2O_3	63.58	60.68	0.03	0.02	0.00	0.03	0.03	0.06	0.03	0.01	0.00	0.03	0.03
Cr_2O_3	0.08	0.11	0.10	0.08	0.06	0.11	0.03	0.00	0.08	0.05	0.03	0.00	0.05
FeO	0.12	0.21	0.07	0.03	0.05	45.29	51.03	49.57	45.68	45.37	36.01	48.97	47.98
MnO	0.00	0.00	0.00	0.03	0.03	0.01	0.29	0.00	1.35	1.27	0.09	0.27	0.35
MgO	0.00	0.01	0.00	0.00	0.00	0.78	0.40	0.63	0.25	0.33	0.23	0.27	0.25
ZnO	0.00	0.00	0.00	0.05	0.00	0.04	0.02	0.15	0.00	0.05	0.04	0.04	0.04
CaO	0.01	0.00	0.00	0.00	0.00	0.00	0.00	0.00	0.00	0.00	0.00	0.00	0.00
Na_2O	0.00	0.01	0.00	0.00	0.00	0.00	0.02	0.00	0.00	0.00	0.00	0.00	0.00
K_2O	0.01	0.01	0.00	0.00	0.00	0.00	0.00	0.00	0.00	0.00	0.01	0.00	0.00
Total	99.81	96.52	98.98	67.12	90.75	99.07	100.26	99.98	92.11	91.76	77.01	100.08	99.92
Formula	5 (O)		2 (O)			3 (O)							
Si	0.975	0.993	0.000	0.000	0.000	0.000	0.000	0.000	0.000	0.000	0.000	0.000	0.000
Ti	0.000	0.001	0.998	0.998	0.999	1.004	0.938	0.954	0.941	0.943	0.998	0.968	0.979
Al	2.029	2.002	0.000	0.000	0.000	0.001	0.001	0.002	0.001	0.000	0.000	0.001	0.001
Cr	0.002	0.002	0.001	0.001	0.001	0.002	0.001	0.000	0.002	0.001	0.001	0.000	0.001
Fe^{3+}	0.003	0.005	0.003	0.005	0.003	0.000	0.179	0.130	0.166	0.162	0.002	0.093	0.058
Fe^{2+}	-	-	0.000	0.000	0.000	0.957	0.919	0.931	0.904	0.903	0.984	0.953	0.963
Mn	0.000	0.000	0.000	0.000	0.000	0.000	0.006	0.000	0.032	0.030	0.003	0.006	0.008
Mg	0.000	0.000	0.000	0.000	0.000	0.029	0.015	0.024	0.010	0.014	0.011	0.010	0.009
Zn	0.000	0.000	0.000	0.001	0.000	0.001	0.000	0.003	0.000	0.001	0.001	0.001	0.001
Ca	0.000	0.000	0.000	0.000	0.000	0.000	0.000	0.000	0.000	0.000	0.000	0.000	0.000
Na	0.000	0.000	0.000	0.000	0.000	0.000	0.001	0.000	0.000	0.000	0.000	0.000	0.000
K	0.000	0.000	0.000	0.000	0.000	0.000	0.000	0.000	0.000	0.000	0.000	0.000	0.000
Total*	3.009	3.004	1.003	1.001	1.001	1.995	2.062	2.044	2.057	2.056	2.001	2.031	2.019

Table 4: Representative EPMA analyses of sillimanite, rutile and ilmenite were found in different rock types.